

**Université Pierre et Marie Curie, École des Mines de Paris  
& École Nationale du Génie Rural des Eaux et des Forêts**

---

**Master 2 Sciences de l'Univers, Environnement, Ecologie  
Parcours Hydrologie-Hydrogéologie**

**Groundwater modeling in karstic  
terrains: example of the Lurbach system**

**Cyril Mayaud**

**Directeur de recherche : Steffen Birk**



**Institute for Earth Sciences  
University of Graz  
Heinrichstrasse, 26  
8010 Graz, Austria**

**Monday, 06<sup>th</sup> September 2010**



## **Abstract**

It is a challenging task to simulate spring responses of karst catchments with the range of distributive modeling software currently available. In spite of the existence of scientific software such as CAVE (Carbonate Aquifer Void Evolution; Liedl et al., 2003), which is useful for modeling transport in karstic conduits and conduits genesis, no corresponding commercial software is available for engineering companies. The goal of this work is to attempt to reproduce the hydraulic behavior of a karst catchment based on widely used groundwater modeling software. The program used here is a free version of Processing Modflow coupled with an additional software called CFP (Conduit Flow Process; Shoemaker et al., 2008) developed by the USGS.

The area selected for the modeling is a 22,4 km<sup>2</sup> well known catchment drained by a stream, the Lurbach, and located about 15 km north to Graz, capital of Styria, Austria. The catchment is divided in two different parts: the upper part lies on an impermeable schist layer and provides allogenic recharge to the lower part, which is constituted of a highly karstified limestone and is also supplied by autogenic input. The research begins with the analysis of measured spring responses. After a first steady state simulation, the models are tested in transient state. Finally, the effects of turbulent flow are examined in simple modeling scenarios.

Particular attention is paid to stay close to reality during the construction of the different models.

**Keywords:** karst catchment, laminar/turbulent flow, Lurbach, single-continuum models, Lurgrotte, groundwater modeling, MODFLOW, MODFLOW-CFP, allogenic/autogenic recharge.

## **Kurzfassung**

Es ist eine große Herausforderung, das Schüttungsverhalten von Karsteinzugebieten mit dem derzeit verfügbaren Spektrum distributiver Modellierungs-Software zu simulieren. Trotz der Existenz wissenschaftlicher Software wie CAVE (Carbonate Aquifer Void Evolution; Liedl et al., 2003), die nützlich ist um den Transport in Karströhren und die Karsthohlrumentwicklung zu modellieren, ist keine entsprechende Software für Ingenieurbüros verfügbar. Das Ziel dieser Arbeit ist es, zu versuchen, das Abflussverhalten eines Karsteinzugsgebiets mit gängiger Grundwassermodellierungs-Software nachzubilden. Das hierbei verwendete Programm ist eine frei verfügbare Version von Processing Modflow sowie die zusätzliche Software CFP (Conduit Flow Process; Shoemaker et al., 2008), die beim USGS entwickelt wurde.

Das Untersuchungsgebiet ist ein 22,4 km<sup>2</sup> großes, sehr gut bekanntes Einzugsgebiet, das durch den Lurbach entwässert wird und etwa 15 km nördlich von Graz liegt, der Hauptstadt der Steiermark, Österreich. Das Einzugsgebiet ist in zwei Teilbereiche untergliedert: der nördliche Teil befindet sich im Bereich von geringdurchlässigen Schiefen und stellt allogene Grundwasserneubildung für den südlichen, von einem sehr stark verkarsteten Kalkmassiv aufgebauten Teil bereit, welcher zusätzlich durch autogene Neubildung gespeist wird. Die Untersuchung beginnt mit der Analyse der Schüttungsdaten. Nach einer stationären Modellierung werden die Modelle in instationären Simulationen getestet. Zum Schluss werden die Auswirkungen turbulenter Strömung in einfachen Modellszenarien untersucht. Dabei wird insbesondere darauf geachtet, dass die Modelle realitätsnah sind.

**Stichwörter:** Karst-Einzugsgebiet, laminare/turbulente Strömung, Lurbach, Einkontinuummodelle, Lurgrotte, Grundwassermodellierung, MODFLOW, MODFLOW-CFP, allogene/autogene Grundwasserneubildung.

## Résumé

La modélisation des débits de sources karstiques à l'aide de modèles maillés est encore très difficile à réaliser actuellement. Malgré l'existence de certains logiciels scientifiques tel que CAVE (Carbonate Aquifer Void Evolution; Liedl et al., 2003), permettant de simuler le transport dans les conduits et la genèse des cavités karstiques, aucun logiciel n'est disponible pour les bureaux d'études. Le but de ce travail est d'essayer de reproduire le comportement d'un bassin versant karstiques avec des logiciels fréquemment utilisés par les bureaux d'études. Le programme utilisé ici est une version gratuite de Processing Modflow couplée à un logiciel nommé CFP (Conduit Flow Process; Shoemaker et al., 2008) développé par l'USGS.

Le bassin versant choisi a une surface de 22,8 km<sup>2</sup> et se trouve à 15 km au nord de Graz, la seconde plus grande ville d'Autriche. Il est divisé en deux parties: la partie amont est composée de schistes imperméables qui fournissent un apport d'eau allogénique à la partie aval, constitué de calcaires hautement karstifiés et recevant aussi un apport d'eau autogénique.

Ce travail commencera par un traitement et l'analyse des données disponibles. Après une première simulation en régime permanent, les modèles seront testés en régime transitoire. Pour finir, la notion d'écoulements turbulents sera introduite au moyen de modèles simples.

Une attention particulière sera donnée à la construction des modèles et au choix des paramètres de modélisation.

**Mots clés:** bassin versant karstifié, écoulements laminaire/turbulent, Lurbach, modèle-un-continuum, Lurgrotte, modélisation hydrogéologique, MODFLOW, MODFLOW-CFP, recharge allogénique/autogénique.

## Acknowledgments

I would here grateful thank people who have given to me the possibility to allow one of my dream: study karst hydrology aboard France, including the opportunity to learn and speak another language than French, and of course, the opportunity to know a new land and a new culture. I will never forget my 6 months stay in Austria and all the people that I have here met.

Thanks particularly to Professor **Steffen Birk**, Dr. **Gerfried Winkler**, Dr. **Thomas Wagner** and the two PhD Students **Bernhard Hubinger** and **Michaela Koch**.

I have also here a thought for the Diplom Ing. **Thomas Reimann** and his internship student **Kim Lompe** of the Technical University of Dresden who works with the source code of CFP for the first and do an internship about the Lurbach for the second.

Thanks also to **Lorenz** and **Gisi** for their friendship and for having spent time with me and to not be offended by my recurrent terrible German errors.

My last thought is for the Dr. **Christoph Rehrl**, which is disappeared in Mars in a tragically mountain accident.

“Presque partout, dans les sources et les rivières des terrains fissurés, on se trouve arrêté, après un parcours plus ou moins long, par des siphons naturels; ils sont formés de *voutes mouillantes*, c'est à dire de murailles rocheuses immergés dans l'eau sur une profondeur et une épaisseur variable, généralement impossible à déterminer.

Ces siphons, véritables vannes fixes, de section restreinte, régularisent dans une certaine mesure le débit des eaux souterraines, qu'ils retiennent pour partie dans les réservoirs ou espaces libres situés en amont.”

**E. A. Martel**, *Sur les siphons des sources et rivières souterraines*, 1896.

## Table of contents

<b>Abstract: English, German, French</b>	<b>2</b>
<b>Acknowledgments</b>	<b>3</b>
<b>Table of contents</b>	<b>4</b>
<b>Introduction</b>	<b>5</b>
<b>1. Presentation of karst aquifers</b>	<b>6</b>
1. Introduction to karst sciences	6
2. Origins of Karstic landscapes	6
3. Karstic aquifers: another form of hydrology/hydrogeology	7
4. Karst and population: preventing groundwater pollution, resources management, protection of people and facilities against floods	11
<b>2. Modeling in karstic aquifers</b>	<b>12</b>
1. Problematic in actual modeling	12
2. Lumped models	12
3. Distributed models	12
Single Continuum Porous Equivalent model (SCPE)	12
Double Continuum Porous Equivalent model (DCPE)	13
Single Continuum Porous Equivalent – Discrete Single Fracture Set model (SCPE-DSFS)	13
Discrete Single Fracture Set model (DSFS)	13
Discrete Multiple Fracture Set models (DMFS)	13
4. Why using MODFLOW here?	13
5. MODFLOW and CFP: simulate turbulent flow in karstic aquifers	13
<b>3. Presentation of the Lurbach system</b>	<b>15</b>
1. Geographical situation	15
2. Geological context	17
3. Measurement device network	18
4. Hydrological behavior of the catchment	19
4.1 Rainfall in the Lurbach catchment	19
4.2 State of the art before this study: Behavior of the Lurbach system until August 2005	21
4.3 Evaluation of the new hydrological data: A new behavior after August 2005?	22
4.4 Potential hypothesis and explanations of the new hydrological behavior	24
<b>4. Modeling with MODFLOW</b>	<b>26</b>
1. Model design	26
1.1 Three-layer model	26
1.2 Four-layer model	28
2. Steady state: Calibration attempt with discharge data of the Steirische Beiträge	30
2.1 Input data	30
2.2 Modeling results	32
Three-layer model	32
Four-layer model	33
3. Transient state	35
3.1 Initial conditions	35
3.2 Hypothetical master recession curves by Behrens et al. (1992)	35

Three-layer model	35
Four-layer model	37
3.3 Flood of August 2005	39
3.4 Events of the field campaign of December 2008	41
4. Attempt to reproduce the new Lurbach behavior	44
<b>5. Modeling with MODFLOW-CFP</b>	<b>46</b>
<b>6. Comparison between MODFLOW and MODFLOW-CFP</b>	<b>48</b>
<b>7. Discussion about the potential intrinsic errors of modeling</b>	<b>49</b>
<b>8. Some suggestions for future work</b>	<b>50</b>
<b>Conclusion</b>	<b>51</b>
<b>References</b>	<b>51</b>

## **Introduction**

The problematic of karst aquifer modeling is of a particular importance because water from karst aquifer concern more than 25% of the world population, and sometimes 100% of the population in area such as south Slovenia.

A better understanding of the hydrology of karst catchments is necessary to improve the distribution and the protection of the water available in karst areas. This is also necessary to prevent the behavior of karstic system during the so-called “Karst Flash Flood” which are recurrent and very destructive around the Mediterranean Sea.

Karstic aquifers are also interesting because they include frequently a duality in their flow regime: the fine matrix is essentially under laminar flow conditions while the conduits draining the karst area are under a turbulent flow regime.

The goal of this work is to test the ability of MODFLOW, a distributive software widely used, to simulate the spring behavior of a well known karst catchment located in Central Styria, Austria.

The duality between laminar and turbulent conditions will be computed with a free-available software called CFP (Conduit Flow Process; Shoemaker et al., 2008) and developed by the USGS.

# 1. Presentation of karst aquifer

## 1. Introduction to karst sciences

The *Karst* is a type of calcareous landforms which was described the first time in a region in the south of *Slovenia* (the Kras in Slovenian, Carso in Italian) by the Serbian geographer *Jovan Cvijić* in 1893 (Das Karstphänomen).

These landscapes are essentially composed of *limestone and dolomite* ( $\text{CaCO}_3$  and  $\text{MgCO}_3$ ) but could be also made in *gypsum* ( $\text{CaSO}_4$ ) such in Western Ukraine, (Klimchouk et al., 1996) or *halite* ( $\text{NaCl}$ ) as the Hyperkarst of the tailing of the Perm salt mine, Ural, Russia, (Salomon, 2006) areas.

In Europa, karst landscapes are present overall, but with a high concentration around the Mediterranean sea. An notable area which begins from Sud-Bavaria (Steinernes Meer between Berchtesgaden and Salzburg), Carinthia and Styria, continue to Slovenia where almost all the land is karstified, Croatia, Bosnia, Montenegro (with the famous Kotor bay), Macedonia and Albania represent a great surface where a great number of people live.

In the world, **10% of the surface of the emerged areas** (Salomon, 2006) are composed of calcareous rocks (30% for France). The population supplied by karst water represents 25% of the world population (Ford and Williams, 2007) and in some lands like Slovenia or Austria more than 50% .

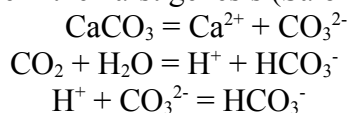
Karst and humans are strongly bound since long time as show the rupestrian pre-historian art in many caves such as Altamira, Lascaux or Chauvet. The caves were an object of devotion and also used as shelters by the early humans. In the middle age, karstic cavities were also used as defenses and escape positions such as the Predjama castle (Slovenia) which is connected with the Postojna cave.

Since the last century, they are essentially used for the tourism, as show caves or for speleology.

## 2. Origin of karstic landscapes

Karst landforms are made by a process named *Karstification* which result of the dissolution the primary rock (limestone and dolomite and sometimes gypsum or halite) under the action of **rainwater** saturated by the  $\text{CO}_2$  of the soils plants roots. The water infiltrates through the fissured and fractured limestone and tend to increase the size of the voids already presents with its acidity. An **hydraulic gradient** between the recharge area and the base level of the outcrop is the second driver which govern the dissolution of the media and the conduits genesis.

The dissolution equations which govern the karst genesis (Salomon, 2005) are:



which gives a global dissolution equation such:



The typical time scale to forms a karstic aquifer under favorable conditions is roughly more than **ten thousand years**.

This action can develop a very complex network of caves relied by conduits which can be gigantic (more than 100 km of conduits network in Postojnska jama, Slovenia) to galleries and rooms which can reach more than 100 m high (Škocjanske jame, Slovenia).

### 3. Karstic aquifers: another form of hydrology/hydrogeology

Because of this constitution of voids, cave and conduits, karstic landscapes are also **efficient aquifers** with a potential **high drainage capacity** and providing a **rapid transport** (until several hundred meters pro hours).

Figure 1 represents a summarizing sketch of a karst aquifer with its main particularities:

The water network begins outside with terranean streams which generally disappear in the unsaturated zone through vertical shafts or swallow holes after encountering a highly karstified layer. The water flows rapidly through the unsaturated zone and reaches the saturated zone. In the aquifer, the stream flows into conduits and resurges at the base level of a hill/escarpment.

In this case, the former base drainage levels are observable in areas where karst landforms crop out and are very developed (such as Peggauer Wand in our investigated area or some cliffs in the Dordogne valley). These old base levels show former active conduits which can become active only if a strong high flood happened and fully saturated the actual drain level.

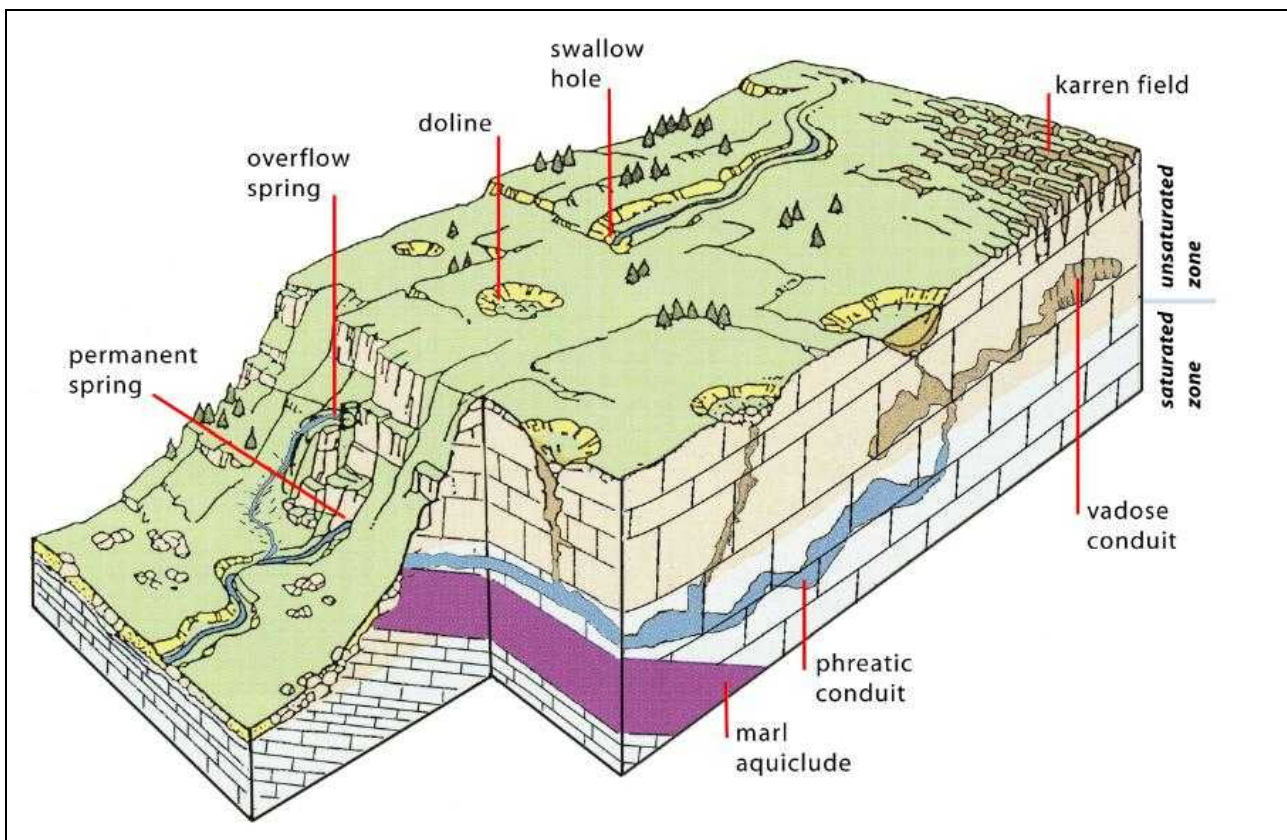


*Figure 1. Conceptual picture of a karst aquifer with its important particularities (Filipponi, modified after Schaer et al., 1998).*

Karst areas present other particularities in their landforms:

- **sinkholes** are natural depressions (which could be named also dolines) formed by suffosion, bedrock dissolution or soil collapse. They can grow up if the dissolution process is still active and encounter other sinkholes to form a mega sinkhole. In some areas they are used as trash deposits.
- **dry valleys** are former surface drained valleys generated after a glacial period. When the glacier has melted, the soil temperature of the valley is still under 0°C and forced the melted water to flow on the valley surface. The stream disappeared in the underground when the soil temperature came over 0°C and allowed the development of a sub-surface drainage network.

- *polje* (crop in Serbian) is a large karst flat depression of several square kilometers surrounded by abrupt landforms. The streams which flows on the surface of a polje disappears in a *ponor*, drains the underground and outlet in a resurgence.

Karstic aquifers can be divided in two different categories in function of the development of the conduits network (Marsaud, 1996):

- *Jurassian karst* if the drainage is the over or at the same altitude of the actual base level. The fracturation degree, lithology and stratification determine a weak resistance again the water flowing and allow the conduits to grow.

- *Vauclusian Karst* if the drainage of the spring is under the actual base level. The fracturation degree, lithology and stratification determine a high resistance again the water flowing and force the drainage network to develop at the base of the outcrop.

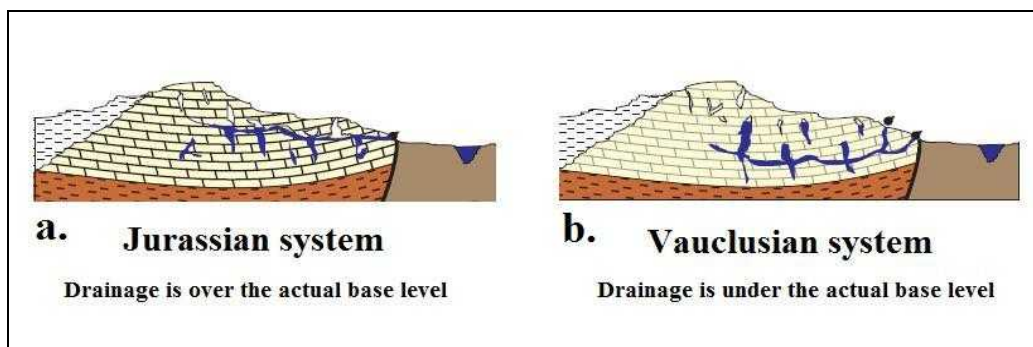


Figure 2. Jurassian (a.) and Vauclusian (b.) system. (from Marsaud, 1996)

Karst aquifers have the particularity to have *two different sort of infiltration* with two different velocities:

- a rapid infiltration through vertical karst conduits, which concentrate a great volume of rainfall and provide to the spring the most volume of water after an event.

- a slow infiltration through small fractures and matrix, where the water accumulate in a area very karstified but lower connected with the main network. This area is located the ten first meters of the limestone.

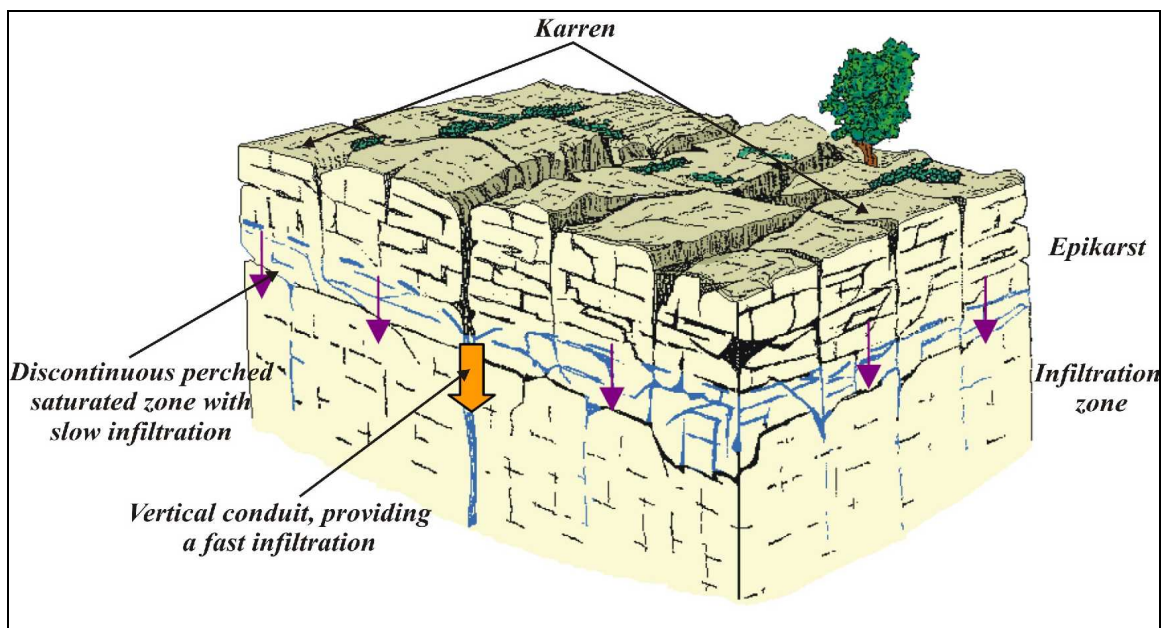


Figure 3. Sketch of the epikarstic zone with the two characteristics infiltrations paths. (Modified after Bakalowicz 2005)

In general, the most of the dissolution happened in this area, because the water stays for long time and became highly concentrate in dissolved CO<sub>2</sub>. This area was highlighted and called **Epikarst** (see Figure 3) after the work of Mangin (1974.a) and supply the karstic aquifer only after heavy rainfall.

The **storage process** in karst aquifers is governed by two trends: the matrix presents a poor capacity of flow and has on the contrary a high storage capacity.

In opposite the conduits have a high potential of drainage but a very poor storage capacity.

Figure 4 present the mains responses of water table during periods under different weather conditions. In a recession period, the matrix provide the essential water volume to the conduits which drain all to the springs. On the contrary, during a recharge period, the spring drains the most volume of water from the conduits whereas the matrix store the water infiltrated through fissures.

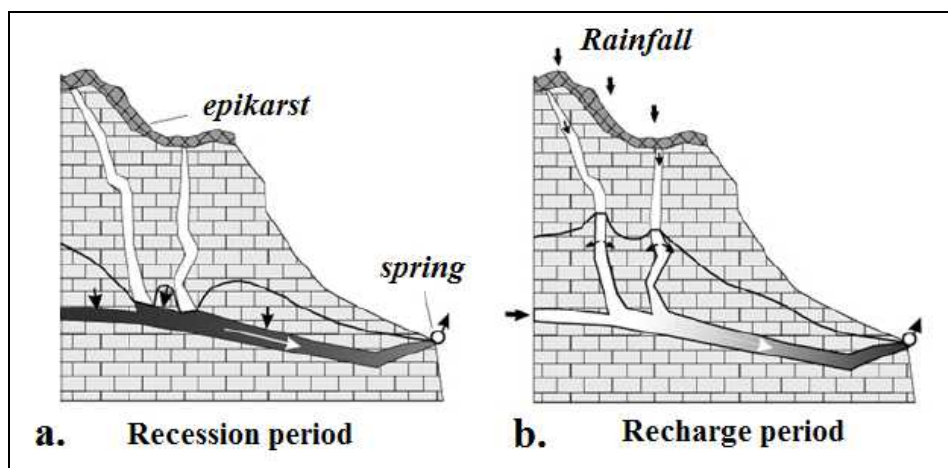


Figure 4. Storage process in a karstic aquifer during a recession period (a) and a rainfall event (b). (redraw after Cornaton et al., 2002)

The porosity of karstic aquifers present another particularity: instead of one or homogeneous porosity like almost all alluvial aquifers, karst aquifers have two or three different porosities (Worthington, 2007):

- the **matrix porosity** has a scale from  $\mu\text{m}$  to mm.
- the second contain **fracture and faults** geometry and has a scale from 10  $\mu\text{m}$  to 10 mm.
- the third is the **conduit or vuggy porosity** and is comprise in a scale between 10 mm to 10 m.

Permeability	Aperture	Travel time	Flow mechanism	Distribution
<b>Matrix</b>	$\mu\text{m}$ to mm	Long	Darcian flow field, laminar	Continuous medium
<b>Fracture</b>	10 $\mu\text{m}$ to 10 mm	Intermediate	Cubic law, mostly laminar, may be non linear component	Localized but statistically distributed
<b>Conduit</b>	10 mm to 10 m	Short	Darcy- Weisbach. Hagen-Poiseuille Open Channel and pipe flow, turbulent/laminar	Localized

Tab.1: Characteristic of the three component of the triple permeability model (White et al, 2005).

Table 1 resumes the mains characteristics of the three different porosities, such as their flow domain and their travel time.

The **matrix flow** is governed by the *Darcy law* (Darnault, 2008) such:

$$Q = -AK \frac{\Delta h}{\Delta l} = \frac{-A \rho g N d^2}{\eta} \frac{\Delta h}{\Delta l}$$

where Q is flow discharge [ $L^3T^{-1}$ ], A is the cross section of the aquifer area [ $L^2$ ], K is the hydraulic conductivity [ $LT^{-1}$ ],  $\rho$  is water density [ $ML^3$ ], g the gravity [ $LT^{-2}$ ],  $Nd^2$  is the permeability [ $L^2$ ] and  $\eta$  is the water viscosity [ $ML^{-1}T^{-1}$ ].

The **fracture flow** is defined by the *Cubic law*, which is derived from the Navier-Stokes equation: C is a constant and f an empirical friction factor which should describe the notion of non-uniform rock fracture in the aquifer and b the aperture of the fracture.

$$\frac{Q}{h} = \frac{C b^3}{f_f}$$

where Q is flow discharge [ $L^3T^{-1}$ ], h the hydraulic head [L],  $f_f$  the friction factor, b the full fracture aperture [ $L^3$ ], and C a single constant.

The **conduit flow** is governed by the *Darcy-Weisbach equation* with the assumption that conduit can be treated as pipe flow (White, 2007).

$$h_f = \frac{f L v^2}{4 g r}$$

where g is the gravity [ $LT^{-2}$ ], f the friction factor, r the conduit radius [L], v the flow velocity [ $LT^{-1}$ ] and L the characteristic length of the conduit [L].

In laminar regime through conduits, the **Hagen-Poiseuille** equation is used:

$$Q = \frac{\pi \rho g r^4}{8 \eta} \frac{dh}{dL}$$

where Q is flow discharge [ $L^3T^{-1}$ ],  $\rho$  is water density [ $ML^3$ ], g the gravity [ $LT^{-2}$ ],  $r^4$  is the conduit radius [ $L^4$ ] and  $\eta$  is the water viscosity [ $ML^{-1}T^{-1}$ ].

The turbulent flow begin when the critical Reynolds number is reach:

$$R_e = \frac{\rho U d_{pore}}{\mu}$$

where U is the mean flow velocity [ $LT^{-1}$ ]  
 $d_{pore}$  is the mean pore size diameter [L]  
 $\rho$  is the water density [ $ML^3$ ]  
 $\mu$  is the dynamic viscosity [ $ML^{-1}T^{-1}$ ]

Figure 6 present the conditions of validation of the Darcy law and Darcy-Weisbach equation with the evolution of the Reynolds number. If  $Re$  is inferior to the critical Reynolds number the flow is laminar while if the Reynolds number is superior to the critical Reynolds number the flow is turbulent.

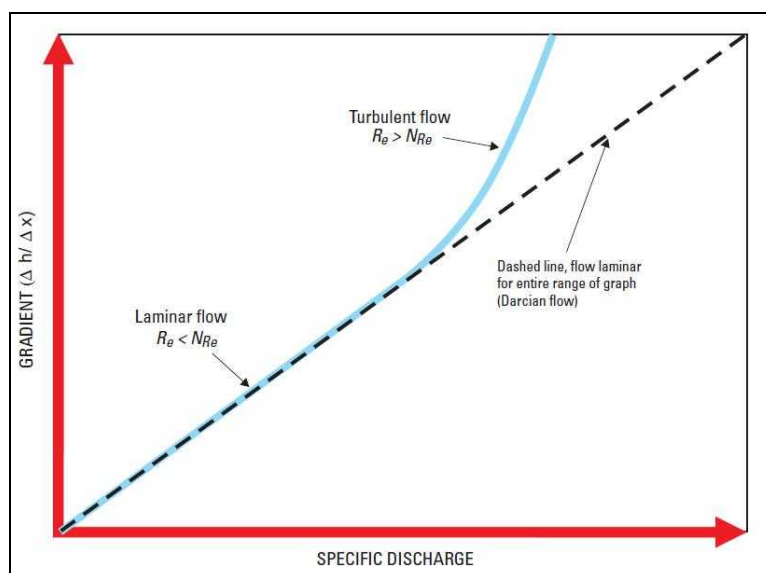


Figure 5. Validity domain of laminar and turbulent flow. (from Shoemaker et al., 2008)

The turbulent flow is easily observable in many show caves where water frequently draw scallop forms to the conduits walls (Salomon, 2006). These forms come from the convection movement made by turbulent flow.

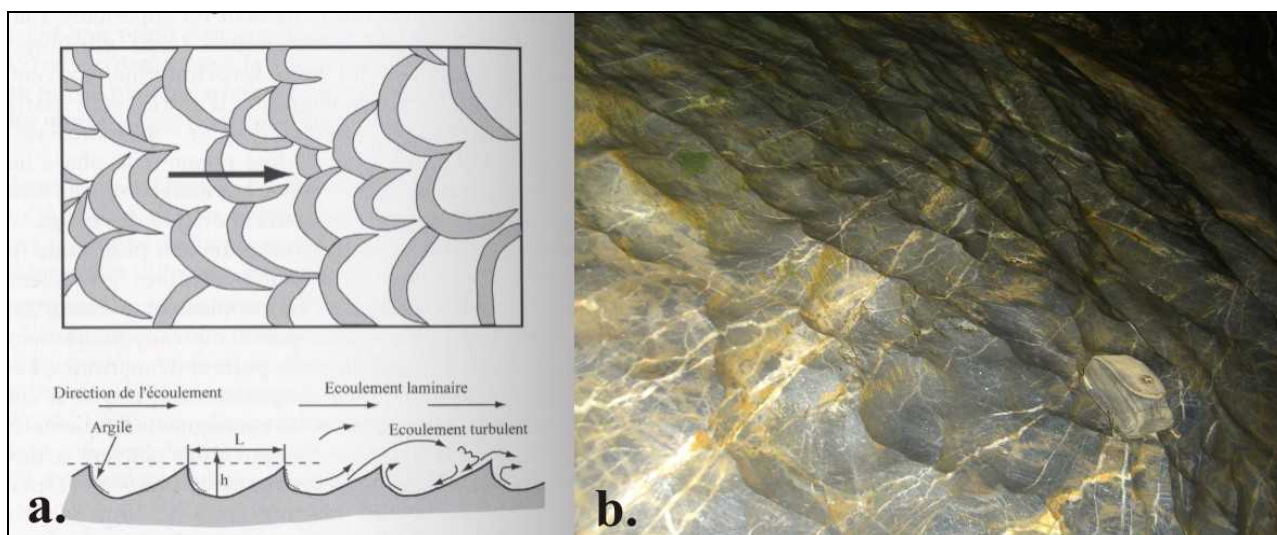


Figure 6. Schematic view of the laminar-turbulent flow duality (a) (Salomon, 2006) and photo of a wall encountering turbulent flow into the Lurgrotte (b). ©Photo T. Wagner

#### 4. Karst and population: preventing groundwater pollution, resources management, protection of people and facilities against floods

Because they are an heterogeneous media with high flow velocities (until several hundred meters per hours), karstic aquifers are very vulnerable to pollution and groundwater contamination. They make attention over a **prevention politic against contamination**. Several methods like PaPRIKA, EPIK or RISKE were implemented in order to answer these problem, with the definition of protection areas and to protect and preserve the resource. They were realized with a consultation of all concerned partners (farmers, scientists, cavers, major and cities administration and population).

Karstic landscapes should also well known and monitored because they can represents a **high risk of flood hazard**. Because the drainage network and the storage capacity is limited than in porous aquifers, karstic conduits network can become very rapidly saturated after strong precipitation

event. They can cause the so called “*Karst flash flood*” (Bonacci et al, 2006), which are very destructive for facilities and cost human yield. A “famous” example is the flood of October 1988 in the city of Nîmes (South of France) where the karst network in the upper part of the city come quickly over-saturated and constrain the water to overflow from the sinkholes to the streets. Karst flash floods are one of the most important hazard in the coastal area around the Mediterranean sea.

## 2. Modeling in Karst aquifers:

### 1. Problematic in actual modeling

Groundwater modeling in karst aquifers is made in order to have a **predictive answer** of the aquifer behavior for event of different intensities and time-scales. The second goal is to determinate the aquifer geometry and the conduits characteristics. The spring responses are simulated and compared with the measured discharge.

### 2. Lumped models

This kind of models are frequently used in karst modeling. They were firstly developed in the domain of hydrology to predict the reactivity of a catchment after a storm event and prevent flood. Theses models can be **rainfall-discharge** models, **discharge-discharge** models, or **rainfall/discharge-discharge** models. They are generally composed of several reservoirs (linear or non-linear) and don't need a definition of the conduits network location. They give only information over the global functioning of the system.

Several authors have made such models which give a very good fit to the discharge curve such Fleury et al., (2007) or Jukić and Denić-Jukić (2009). The great advantage of these models is that they require very few input parameters and no knowledge of the conduits/cave network.

### 3. Distributed models

Distributed models allow a definition of heterogeneous zones. They are based on the **finite difference** or **finite element** methods. They require more knowledge of the computed catchment than global models. Distributed models can be divided in two categories:

- discrete models: which define flow into individual fault and conduits.
- continuum models: which define heterogeneous structure as spatial continuum parameters field.

The description of the following distributed models come from Teutsch and Sauter (1991) and Sauter et al., (2006).

**Single Continuum Porous Equivalent model (SCPE)** follows the definition of the Representative Volumic Element (RVE) and allow only few contrast in hydraulic conductivity.

**Double Continuum Porous Equivalent model (DCPE)** can simulate hydraulic effect of karst conduit without exact knowledge of their position and geometry. In the DCPE model the conduit network and the matrix are defined as two different continuum which can interact each other. The transfer between the matrix and the conduit network is defined as:

$$Q_{ex} = \alpha_{ex} (H1 - H2)$$

where  $\alpha_{ex}$  [ $L^{-1}T^{-1}$ ] describe the transfer coefficient between the two continuum.

The advantage of the double continuum approach is the good description of the dual behavior of the karst conduits.

**Single Continuum Porous Equivalent – Discrete Single Fracture Set model (SCPE-DSFS)** is the coupling of a SCPE continuum with a discrete conduit network.

**Discrete Single Fracture Set models (DSFS)** is constituted of a matrix and a fault/fractures network.

**Discrete Multiple Fracture Set models (DMFS)** are not really different from DSFS models. They just include a multiple fracture set.

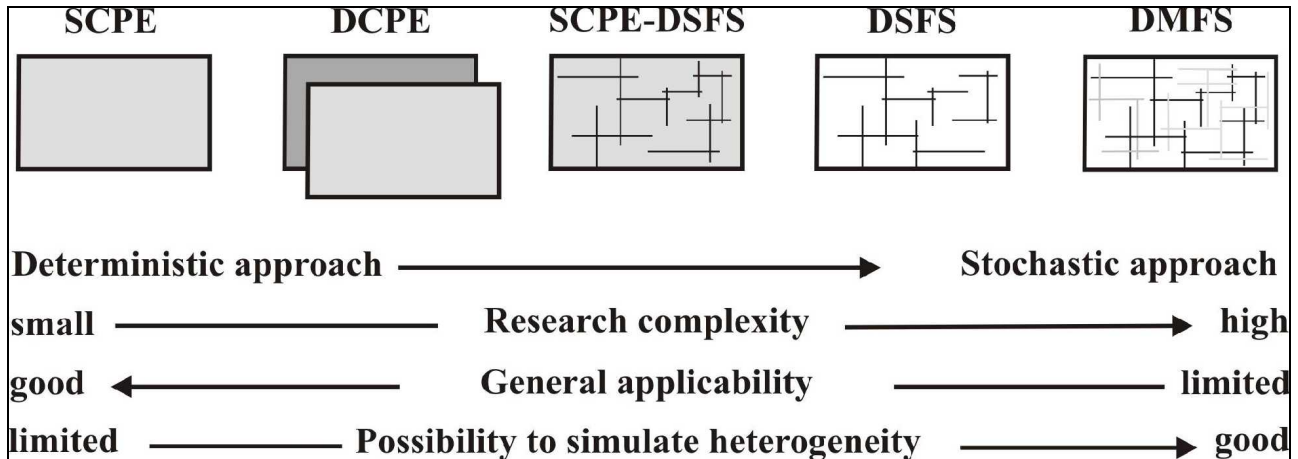


Figure 7. The different karstic models. SCPE (Single Continuum Porous Equivalent) DCPE (Double Continuum Porous Equivalent) SCPE-DSFS (Single Continuum Porous Equivalent – Discrete Single Fracture Set) DSFS (Discrete Single Fracture Set) DMFS (Discrete Multiple Fracture Set). (from Sauter et al., 2006)

#### 4. Why using MODFLOW here?

In this work, the modeling of the Lurbach catchment was made with MODFLOW 96 in laminar flow and MODFLOW 2000 with CFP for the turbulent flow. An important question here concerns the relevancy of the choose of MODFLOW and no other modeling software.

MODFLOW presents the advantage to have a total free version available on its website, which can easily coupled with CFP. This is very useful for students and engineering companies where it is very used. MODFLOW has also a graphic interface very easy for user.

#### 5. MODFLOW and CFP: simulate turbulent flow in karstic aquifers

CFP (Conduit Flow Process) is a software developed by the USGS (Shoemaker et al, 2008) in order to simulate turbulent flow in karstic aquifers. It is based on the source code of former software such as CAVE (Conduit Aquifers and Voids Evolution) (Liedl et al., 2003) which were improved and integrated to MODFLOW with Fortran. This software is free-available on the Web-page of the USGS (<http://water.usgs.gov/software/lists/groundwater/>). CFP should be combined with other groundwater software like MODFLOW, MODBRAC or FEFLOW to simulate turbulent flow.

When CFP is used with MODFLOW the user can only simulate with MODFLOW 2000 and the groundwater equation can be solved only with the solver SIP (Strongly Implicit Procedure). The user need to compute firstly the model under laminar conditions with MODFLOW and then to call CFP for the computation in turbulent flow.

After each computation, a file named *turblam.txt* is created in the model folder where the flow regime of each cell is written. If the value of the cell is equal to 0 the flow is laminar. If the cell value is equal to 1 the flow is turbulent in the right direction and laminar in the front direction. If the cell value is 2 the flow is turbulent in front face and laminar in right face. If the cell is equal to 3 the flow is turbulent in right and front face.

CFP was initially defined in three different modes: MODE 1, MODE 2 and MODE 3 which allow to simulate turbulent flow in different groundwater models.

CFP Mode 1 (CFP M1) was developed for coupling the traditional flow equation with discrete network of cylindrical pipe, whereas CFP Mode 2 (CFP M2) define preferential flow layers in the model, where the laminar and turbulent flow could switch each other, in function of the hydraulic conditions. CFP Mode 3 (CFP M3) allows simulation of flow in conduits flow pipe and preferential flow layers (Shoemaker et al., 2008).

A new mode named CFP M4 (CFP Mode 4) was developed in 2010 (Reimann et al, 2010) because the former CFP M2 presented an error in the transition between laminar and turbulent flow (the solution was dependent of the number of iterations). This new mode CFP M4 is an improvement of CFP M2 and allows to simulate turbulent flow in preferential flow layers independently of the iterations number.

CFP M4 was the only mode used to compute turbulent flow in this work. Input data of CFP M2 and M4 need only a MODFLOW 2000 model computed with the solver SIP. As in MODFLOW, CFP need a name file (which can be a copy of the MODFLOW name file) to call all packages of the software for the computation.

The turbulent flow should defined in a new text file which will be also called by the CFP name file.

In the new file, the number of preferential flow layers in the model should be written with the number of each involved layer. For each layer, the user must give a water temperature and two critical Reynolds number (lower and upper critical Reynolds number).

Then the user can firstly compute in laminar with MODFLOW 2000 and after with CFP.

### 3. Presentation of the Lurbach system

#### 1. Geographical situation

The study site is a 22,8 km<sup>2</sup> catchment located 15 km North of **Graz**, capital of **Styria** and second biggest city of **Austria** (Figure 8). This region is part of the **Highland of Graz**, and belongs to the **Central Styrian Karst**.



Figure 8. Location of Graz and Lurbach catchment.

The catchment is delimited by several important features: the **Mur** river flows in a North-South direction and is a 500 meters wide valley at the West border of the catchment. A major 300 m high limestone escarpment called **Peggauer Wand** (Figure 11) is located on the Eastern side of the **Mur valley**, along the town of **Peggau** (400 m asl., local base level of the area) and is the most important feature of the West part of the catchment.

The East side is delimited by a hill range with several summits such as the **Windhofkogel** (1.064 m asl) or the **Rechbergkogel** (1.020 m asl) and form also the watershed. The highest summit of the area is called **Fragnerberg** (1.109 m asl, Figure 9) and is located North of the village of **Neudorf** (790 m asl). The city of **Semriach** (709 m asl, Figure 9) is in the center of the catchment.

The North side of the area under investigation is delimited by a stream called **Badlgraben** (Figure 9), which flows in a narrow valley from the East to the West.

The **Tanneben massif** (Figure 9) begins on the top of the Peggauer Wand and is located between Semriach, the Mur and the Badlgraben valleys. It is a 8,3 km<sup>2</sup> limestone plateau constituted of densely wooded hills. The main summits are the **Hochglaserer** (910 m asl) and the **Krienzerkogel** (906 m asl). A farm called **Erthube** (745 m asl) is located close to the edge of the Peggauer Wand. Several sinkholes, caves, vertical shafts and a dry valley called **Brunngraben** are the main features. In the South of the Tanneben massif, a little stream called **Mitterbach** constitutes the southern border of the catchment.

In the East of the Badlgraben valley and the Tanneben massif rises a 891 m high hill called **Eichberg** (see Figure 9), which has the particularity to have a well developed network of sinkholes. Most of them are inactive today (mostly plugged with sediments). However, three sinkholes located North and North-West from Eichberg hill are still active (Figure 9). They are called **Katzenbachschwinde** (on the North-West side), **Eisgrube** and **Neudorferschwinde** (on the North side).

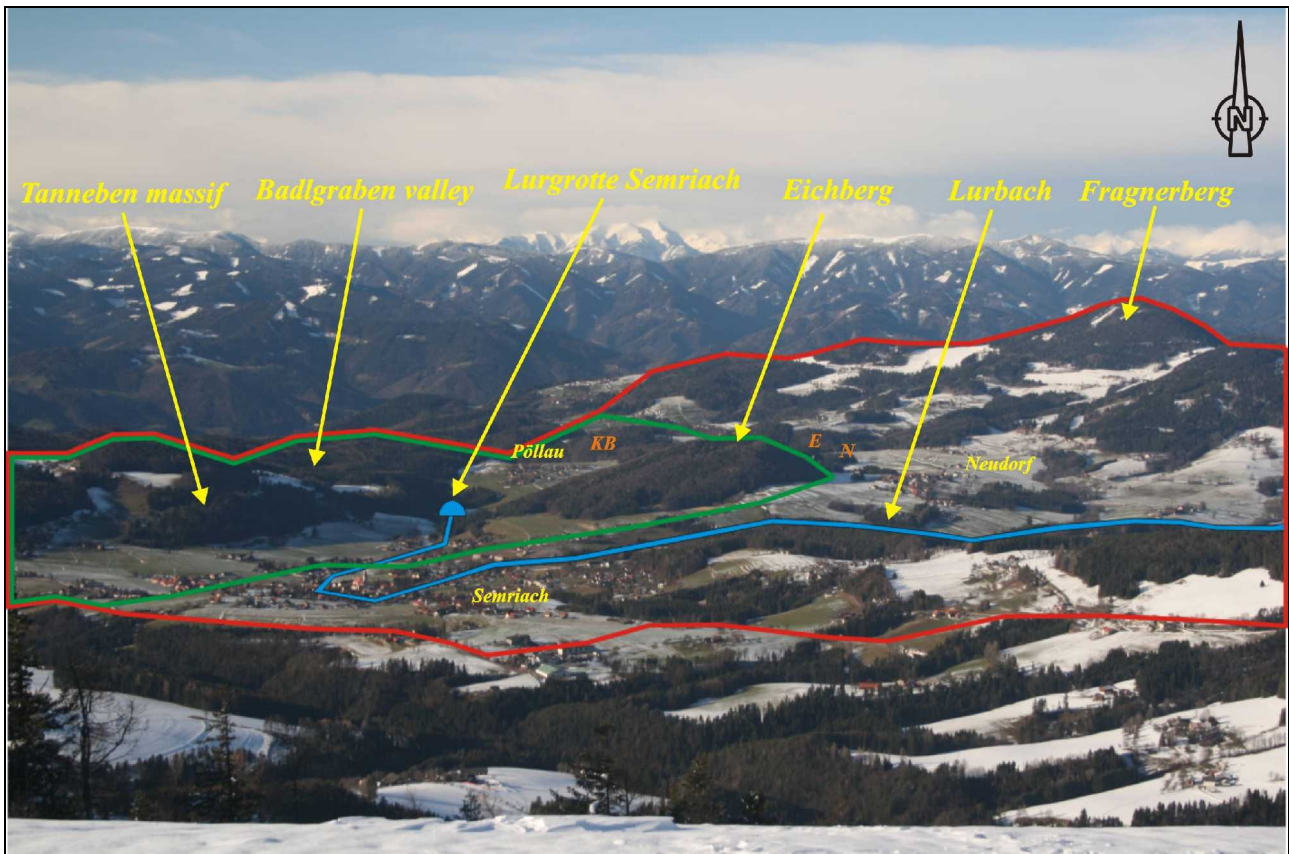


Figure 9. General view of the region of interest taken from the Schöckl mountain (1.445 m asl). The regional most important features are here presented. The red line delineates the Lurbach catchment, whereas the green line represents only the Tanneben massif and the Eichberg hill. The orange letters represents the location of the Katzenbachschwinde (KB), Neudorferschwinde (N) and Eisgrube (E) sinkholes. © Photo: M. Schneider

The hydrographic network is constituted of a little creek called **Lurbach** (see Figure above) with his tributaries streams. The Lurbach originates in the East side of the catchment at an altitude of about 850 m asl. and drains the study region in a South-West direction towards the Mur valley. After the city of Semriach, the stream turns into the North-West direction, flows in a 500 m long gorge like valley, and begins to loose within several sinkholes and vertical shafts located between the sewage plant of Semriach and a dam. The rest of the stream disappears in sinkholes after the entrance of a cave called **Lurgrotte** (629 m asl, see Figure below).

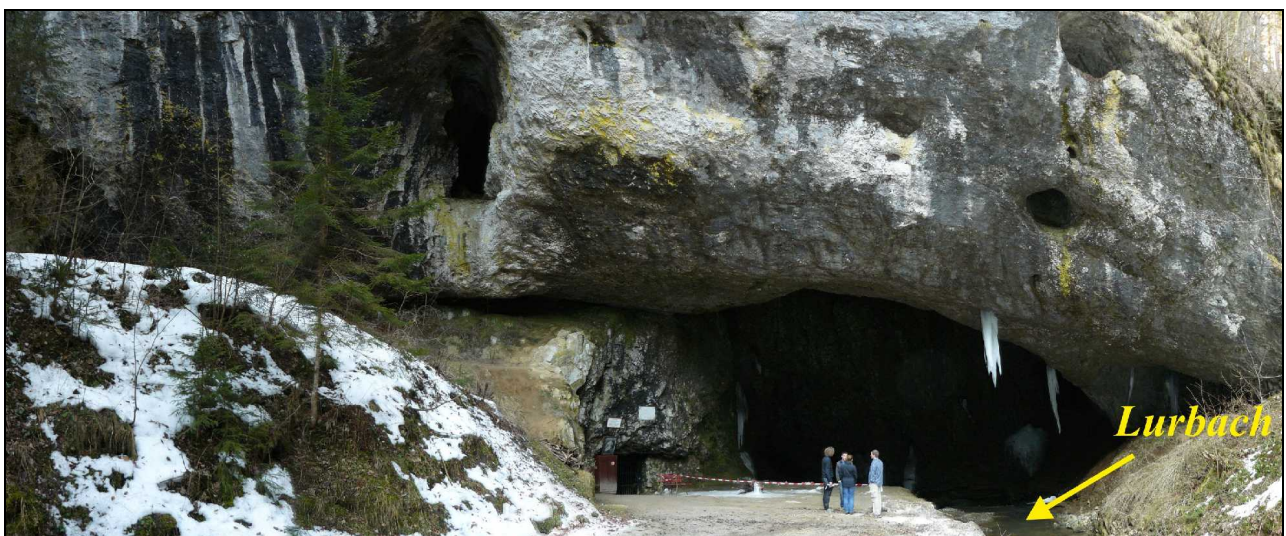


Figure 10. Upper entrance of the Lurgrotte cave located in the vicinity of Semriach (see Figure 9).

This cave is a famous show cave in Austria. It has two entrances, one at the foot of the Peggauer Wand (Figure 11) and the other near Semriach, at the East border of the Tanneben plateau (see Figures 9 and 10). The Lurbach flows in the subsurface through the Tanneben plateau and resurges in two places at the foot of the Peggauer Wand, the so-called *Schmelzbach outlet* and *Hammerbach spring* (see Figure below).



**Figure 11.** Photo of the Peggauer Wand with the Schmelzbach outlet and Hammerbach spring. The entrance of the Lurgrotte side Peggau is represented by the green circle. Caves which indicate the former base level of the karst system in the Peggauer Wand are visible. The Schmelzbach flows currently through an artificial exit tunnel. The former Schmelzbach outlet is 4 meter higher, and is presently used as entrance of the Lurgrotte Peggau.

An important part of the conduit network of the Lurgrotte is known and accessible (the connection between the side of Semriach and the side of Peggau is mapped). On the contrary, the Schmelzbach and Hammerbach network are only indirectly investigated because these parts are not (yet?) accessible by cavers/speleologists. Therefore, hydrological behavior of these (interconnected) systems needs to be studied in much detail to draw conclusions on the character of this subterranean complex drainage network. By studying the recharge-discharge behavior, a better understanding of the geometric properties and possibly their spatial distribution is intended.

## 2. Geological context

The area is constituted of two different geologic units: **permeable and karstified limestones** and **impermeable and non karstified schists**.

In general, the upper part of the Lurbach catchment (14,5 km<sup>2</sup>) is poorly karstified (except the part near the town of Blasenlois, where limestone crop out) whereas the lower part (Peggauer Wand, Tanneben and Eichberg) shows a very high degree of karstification (Figure 12).

The first geological unit is dated from **Paleozoic** and can be divided in two parts.

The **Schöckel Group** is composed of two major layers: the **Schöckel limestone** which is a grey and grayish-blue to white very dense limestone (represented in blue on Figure 12). The thickness of the layer is about 100 m, but some areas can be more thick in the studied zone. This limestone is very pure (more than 97% CaCO<sub>3</sub>) and only few parts are dolomitized.

The second layer is called **Arzberg formation** (in green in Figure 12) and is constituted of a serie of dark limestones and carbonatic schists. The average thickness is between 200 and 300 m.

The second group is called **Passail Group** and is an epizonic-metamorphic, vulcanogenedimentary sequence with a thickness of more than 1000 m.

The **Rannach Facies** (Schwinner 1925, Maurin 1954) is located in the vicinity of the Krienzerkogel and is constituted of friable sandy schists.

**Quaternary clastic sediments** are found in the Mur valley (beige color in Figure 12). They are composed of gravel and constitutes the Würm terraces of the river. They have a thickness of about from 20 to 40 m and fill a trough in the Mur valley.

**Neogene sediments** (Schwinner 1925, Maurin 1954) are also present on the Semriach Basin and Tanneben plateau. They are composed pebbles and bluish green argillaceous-rich loam mixed with rests of fossils plants.

The main direction of the **fault network** is North-South.

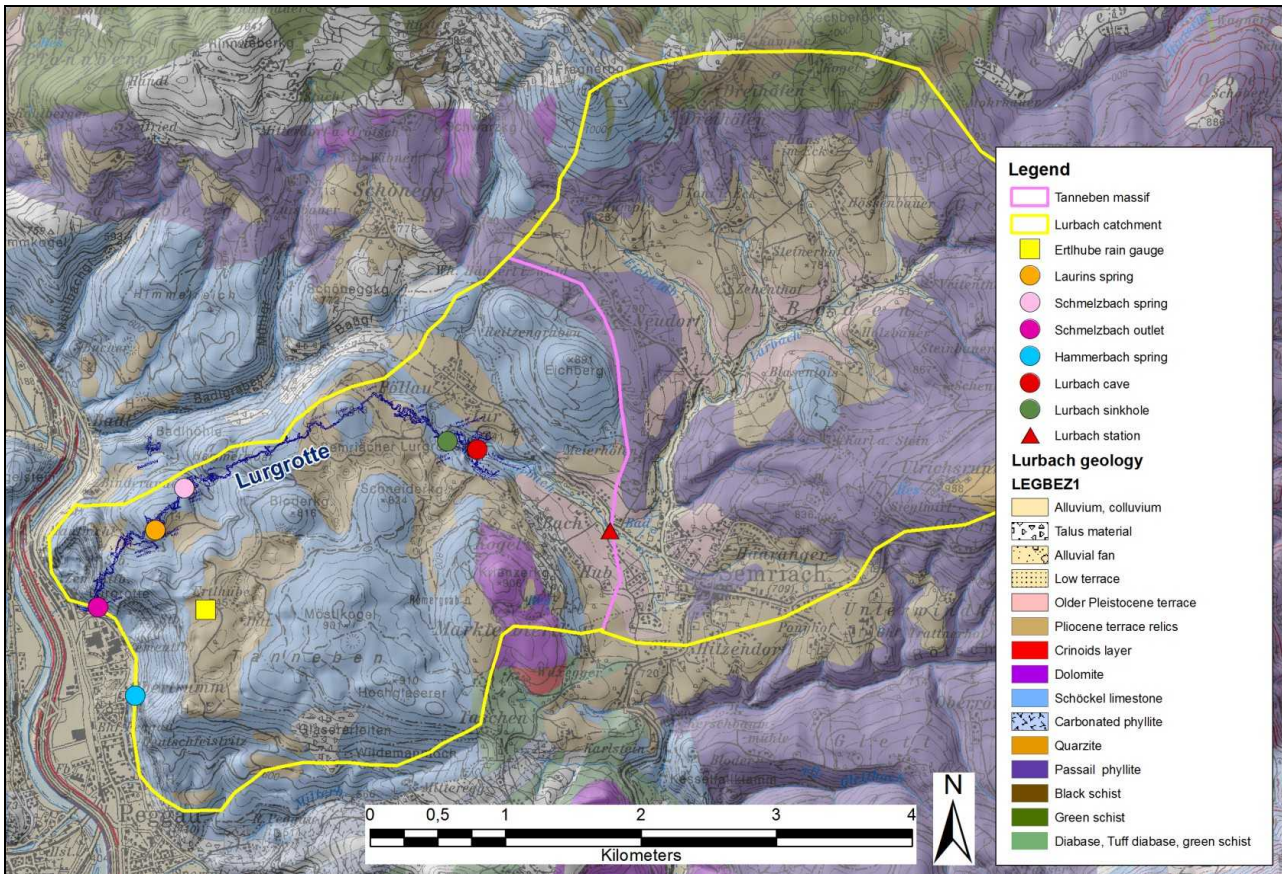


Figure 12. Geological context and monitoring network of the Lurbach catchment (modified after Oswald, 2009).

### 3. Measurement device network

The investigation area disposes of some measurement devices which allow a (nearly) complete monitoring of the hydrological behavior of the Lurbach system (see also the map of Figure 12).

Two rain gauges are installed in the area in order to measure daily precipitation. One is located in the vicinity of Semriach (not indicated in Figure 12), whereas the other is in **Erthube** (Figure 13.a), on the Tanneben massif.

The discharge of the Lurbach is measured at two points. The first device is located at **Lurbach station** (Figure 13.b), downstream of Semriach, at the border between limestones and schists. The second monitoring station is named **Lurbach cave** and situated before the disappearance of the stream into the Lurgrotte. This allows to quantify the volume of allogenic water supplied by the upper Lurbach catchment and the water which infiltrates through the stream bed before the total disappearance of the Lurbach into the cave.

Two discharge stations are located on the western edge of the Tanneben massif (Figure 11), in a small concrete building for the Hammerbach spring and at the entrance of Lurgrotte Peggau for the Schmelzbach creek (indicates as Hammerbach spring and Schmelzbach outlet in Figure 12).



Figure 13. Rain gauge of Ertlhube (a) and Lurbach station (b).

The data set used in this work was taken from a 2 month field campaign in winter 2008, where meteorological data and the rates of the four sampling stations were measured (Oswald, 2009). We dispose also of a 14 years discharge set of the Hammerbach creek. In the end of July, we have got precipitation data of seven different rain gauges (include Semriach and Ertlhube rain gauge) located around the area under investigation with a monitoring period of about 40 years (between 1965 and 2008). These data were provided by the Austrian federal state government and the Water Department of the Joanneum Research Institute of Graz.

The Hammerbach data are available for a greater time span than the Schmelzbach data because the hydrological behavior of the Hammerbach is more stable than the Schmelzbach (as described in the following), where the water discharge can strongly vary and cause some measurement errors and destruction of stations. The Lurbach station and Lurbach cave station can also be disturbed by the change of temperature in winter which can cause the development of ice caps on the pressure sensor (Oswald, 2009). These problems are reduced for the Hammerbach and Schmelzbach stations because they are located near the entrance of the cave and in a house where temperature reach rarely freezing condition.

The investigated area has unfortunately **no observation boreholes** which could give an idea of the groundwater surface in the Tanneben massif. The only assumptions can be made with the field observations of speleologists and an available sinkhole network map (Maurin, 1952). The water table is close to the active lower level of the cave system.

#### 4. Hydrological behavior of the catchment

In the following, we denominate the system between Lurbach spring, Schmelzbach outlet and Hammerbach spring under the appellation of **Lurbach system**. If the name Lurbach is written alone (without the word system), it means that the word concerns only the Lurbach surface stream from its spring to the Lurgrotte sinkholes.

##### 4.1 Rainfall in the Lurbach catchment

In the area, precipitations are characterized by snow fall in winter (maximum of 54 days of snow cover and two days with more than 50 cm) and intense storms in summer (Behrens et al, 1992).

The precipitation rate is higher in summer (about 119 mm in June due to the high frequency of storm events) than in winter (about 40 mm in December). During the year, a mean of 262 days are without rain (Behrens et al, 1992). The record daily rainfall was measured in July 1975 with 93,5 mm.

A mean annual air temperature of 8,5°C was measured between 1971 and 1980 in the station of Frohnleiten (15 km North of Peggau at 440 m asl).

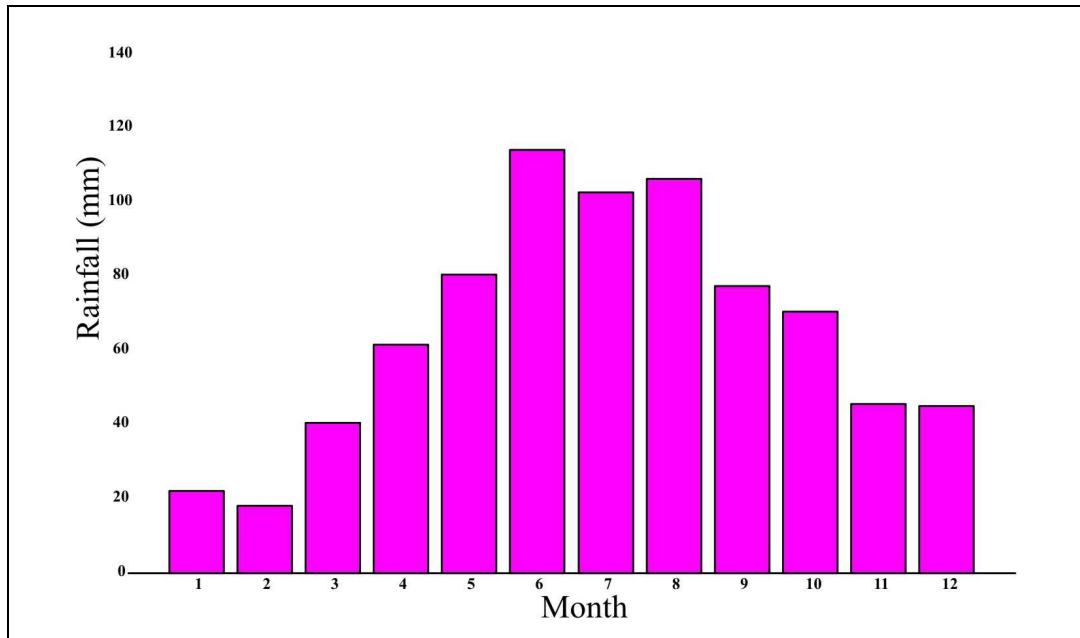


Figure 14. Monthly precipitations above Tanneben massif based on data from the years 1995-2004.

During 1995 and 2004, the annual mean precipitation in the region was 843 mm.y<sup>-1</sup> with a maximum of 1001 mm.y<sup>-1</sup> in 1996 and a minimum of 548 mm.y<sup>-1</sup> in 2001. These data are in agreement with the data presented in Behrens et al, reporting respectively from 1971 to 1980 a mean of 880 mm.y<sup>-1</sup>, a maximum of 1.351 mm.y<sup>-1</sup> (which is also the maximum value between 1971 and today) and a minimum of 669 mm.y<sup>-1</sup>.

The upper part of the catchment is supplied by **allogenic** recharge, where all rainfall is collected by the Lurbach creek. The Tanneben massif (included the Eichberg hill) receives water from the upper Lurbach catchment and an **autogenic** recharge composed of the effective rainfall which infiltrates through the limestone layer. If we considers the classification of Marsaud (1996), the Lurbach system can be denominated as a **binary system** (Figure 15.b).

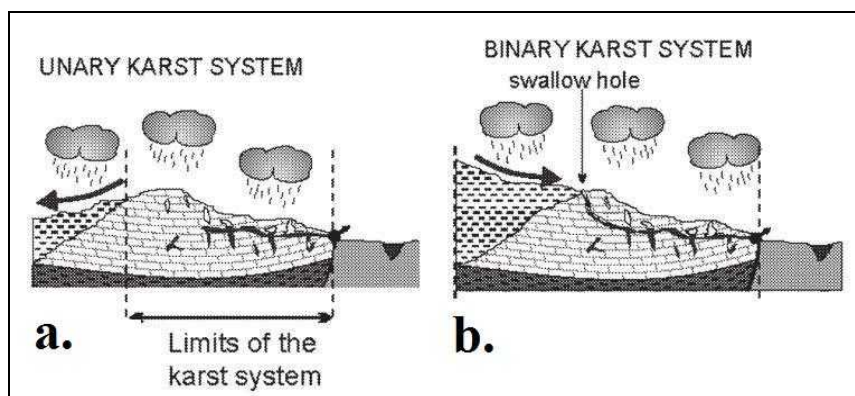


Figure 15. Unary system (a) with only autogenic recharge and binary system (b) with allogenic and autogenic recharge (such as the Tanneben massif). ©from Marsaud 1996

## 4.2 State of the art before this study: Behavior of the Lurbach system until August 2005

The behavior of the Lurbach system varies strongly with weather conditions and season (Behrens et al, 1992).

By **severe drought conditions**, the Lurbach can totally disappears 100 m before it enters the Lurgrotte and supplies only the Hammerbach spring (Behrens et al, 1992). The Schmelzbach is recharged by autogenic recharge through the Tanneben massif, by the water from the sinkholes in vicinity of the Eichberg hill and by the *Laurins spring*, a little stream which appears in the Lurgrotte downstream of the Schmelzbach spring (represented in Figure 12) and provides also autogenic recharge water from Tanneben.

By **normal water conditions**, the Lurbach flows from the spring located in the upper part of the catchment to Semriach. Five hundred meters after the town, the Lurbach enters into the karstified area (at the point called Lurbach station in Figure 12). It flows about 500 m in North-West direction and comes across the dam after the sewage plant of Semriach (see Figure 19), where a part of its water infiltrates through sinkholes. Finally, the stream enters in the Lurgrotte and disappears after some meters into inaccessible sinkholes.

The water of the Lurbach passes through the Tanneben massif and resurges at the Hammerbach spring. The water of Schmelzbach outlet is the sum of the Schmelzbach spring which comes only from infiltration into sinkholes located in the vicinity of Eichberg such as the Katzenbachschwinde, the Eisgrube and the Neudorferschwinde, from the Laurins spring and from an autogenic recharge through the Tanneben massif.

During **high flood periods**, the water discharge of the Lurbach can increase very rapidly (up to  $15 \text{ m}^3\text{s}^{-1}$  at the Lurbach station) and most of it directly sinks in the main conduit of the Lurgrotte supplying the Schmelzbach outlet at exit of the cave system. The Hammerbach spring does not exceed  $2 \text{ m}^3\text{s}^{-1}$  which proves that the Hammerbach network can become rapidly fully saturated after a heavy storm event.

A **non-permanent connection** between the Hammerbach and the Schmelzbach was deduced by the use of fluorescent tracers such as Eosine or Uranine (Behrens et al, 1992). A threshold effect is reached when the water discharge of the Hammerbach spring increases above approx.  $200 \text{ ls}^{-1}$ . A part of the water of the Hammerbach system is transferred over to the Schmelzbach system.

The presence of supposed sinkholes and caves along the Lurbach stream (such as the *Blasloch*, a 600 m long cave discovered in 1990, located in the Tanneben plateau not far away of the upper Lurgrotte entrance), indicates that a part of the Lurbach water percolates/infiltrates before the entrance into the Lurgrotte (Figure 19.c). These losses of water are clearly observed by normal water conditions in the data of a field campaign from December 2008 (Oswald, 2009).

Discharge ( $\text{ls}^{-1}$ )	Lurbach	Schmelzbach	Hammerbach
<b>Drought</b>	4	15,4	33
<b>Mean annual discharge</b>	141	82,7	193
<b>Flood</b>	15.300	11.400	2.000
<b>Monitoring period</b>	1965-1973, 1987-1989	1965-1970, 1983-1989	1965-1975, 1983-1989

*Tab.2: Discharge rates of the Lurbach system with the monitored periods (Behrens et al, 1992). The discharge of the Lurbach is measured at Lurbach station. The Schmelzbach data are the sum of the Schmelzbach spring and the Laurins spring discharge, measured at the entrance Lurgrotte Peggau (Schmelzbach outlet, Figure 11).*

The Table 2 presents the Lurbach system water discharge rates under various weather conditions during the indicated monitored periods. As mentioned previously, the Schmelzbach behaves totally different by drought or by high floods periods (ratio of 760 between the two measured discharges). The behavior of the Hammerbach is more stable (ratio of 61) but seems rapidly fully saturated by high flood events .

Several tracer experiments presented in Behrens et al have determined that the water supplied by the upper part of Lurbach catchment (mean annual discharge measured with the tracers of  $184 \text{ ls}^{-1}$ ) is separated in two components after its entrance in the Lurgrotte: under normal weather conditions a major part contributes to the Hammerbach ( $122 \text{ ls}^{-1}$ ) and the rest to the Schmelzbach ( $62 \text{ ls}^{-1}$ ). The precipitation above the Tanneben massif accounts for the remaining contribution of the discharge measured of the Schmelzbach outlet and Hammerbach spring (Behrens et al, 1992).

The tracer experiments have shown **no evidence for a conduit connection between the Hammerbach and Schmelzbach network and the unconfined alluvial aquifer of the Mur valley**. However, a diffuse infiltration into the Mur valley through fissured limestones cannot be excluded (Behrens et al, 1992).

As the system responds differently for various types of hydraulic conditions, an evolution of the catchment area with the weather conditions is observed.

By normal and drought weather conditions, the Tanneben massif seems to be divided in **two distinct unconnected catchments**: one part drains the Lurbach water and Tanneben infiltration to Hammerbach spring, whereas the other drains water of Eichberg area and infiltration from Tanneben to Schmelzbach outlet. If the discharge of the Hammerbach increases above the threshold of  $200 \text{ ls}^{-1}$ , a **connection becomes active between these two areas** and water is transferred from the Hammerbach system to the Schmelzbach system.

During extreme high flood events, the Tanneben works as a global catchment and no distinction between the Schmelzbach and Hammerbach area can be done because all is connected. However, a direct connection of Lurbach and Schmelzbach via the Lurgrotte cave main conduit becomes evident.

**It is clear that further investigations are needed in order to improve the knowledge of the water transfer between the Lurbach, Hammerbach and Schmelzbach.**

#### **4.3 Evaluation of the new hydrological data: A new behavior after August 2005?**

In the Hammerbach discharge data from 1995 to 2009, a change in the behavior of the Lurbach system is observed. After August 2005 (where a maximum flood discharge of  $1.623 \text{ m}^3\text{s}^{-1}$  was recorded at the Hammerbach spring the 21 August 2005), the characteristics of the system changed and the Hammerbach spring does not show anymore events with rates above  $500 \text{ ls}^{-1}$  although such floods were previously observed on average one per year (Figure 16).

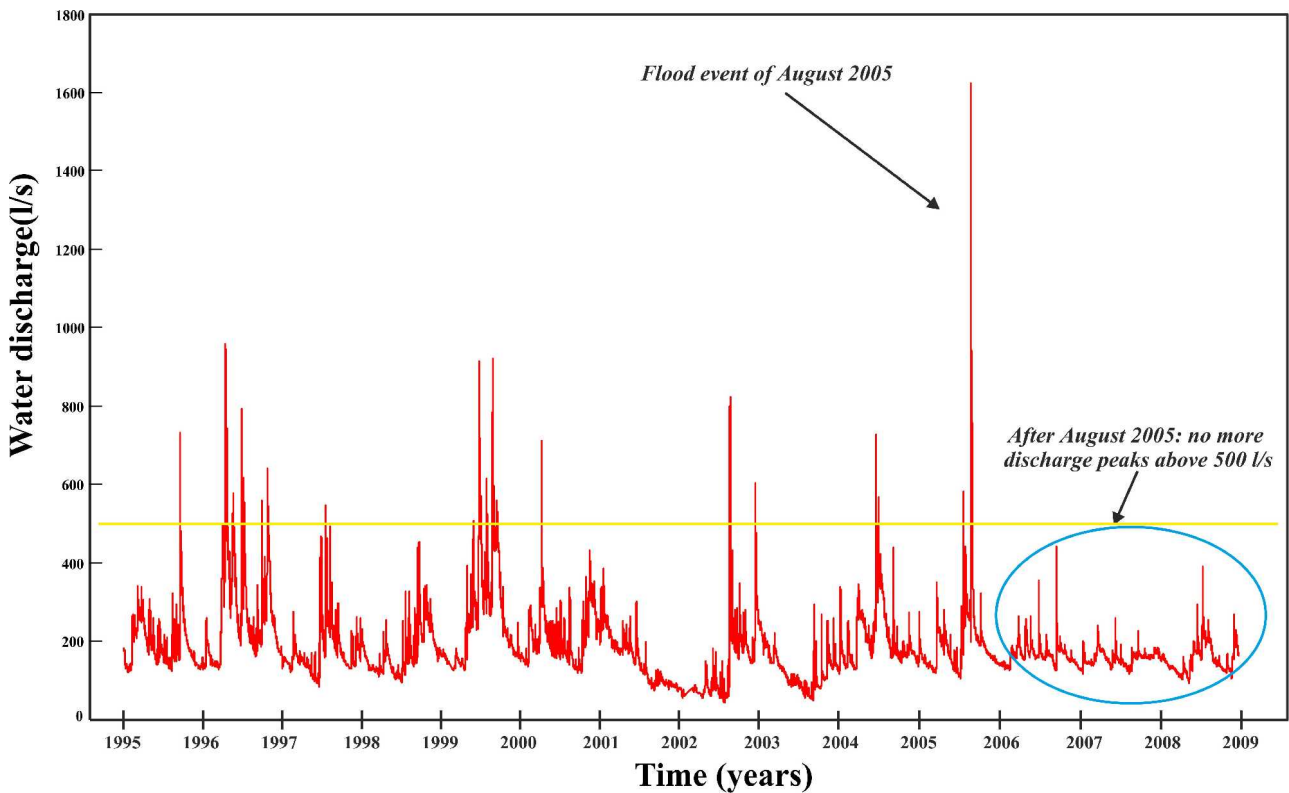


Figure 16. Hammerbach discharge between 1995 and 2009.

After the first flood peak a second delayed peak at  $792,5 \text{ ls}^{-1}$  is observed the 26 August 2005 at 23:30 (see Figure above). It is probably due to the slow drain of a plugged reservoir, or a branch dam rupture in the upper Lurbach or a new event combined with the delayed infiltration waters of the first strong event.

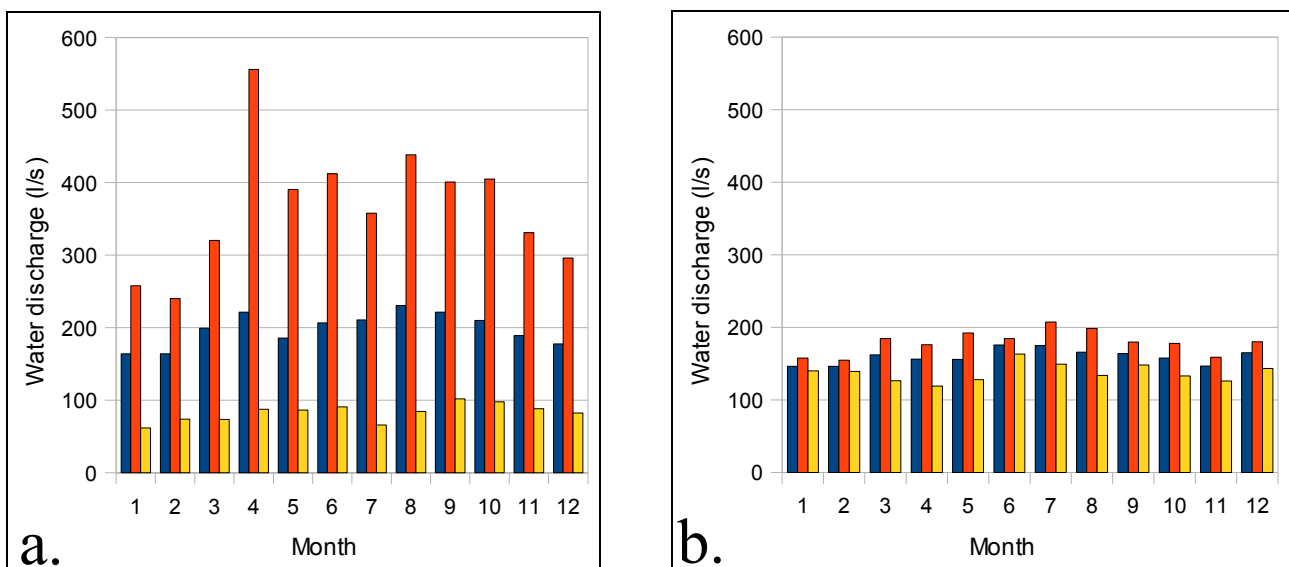
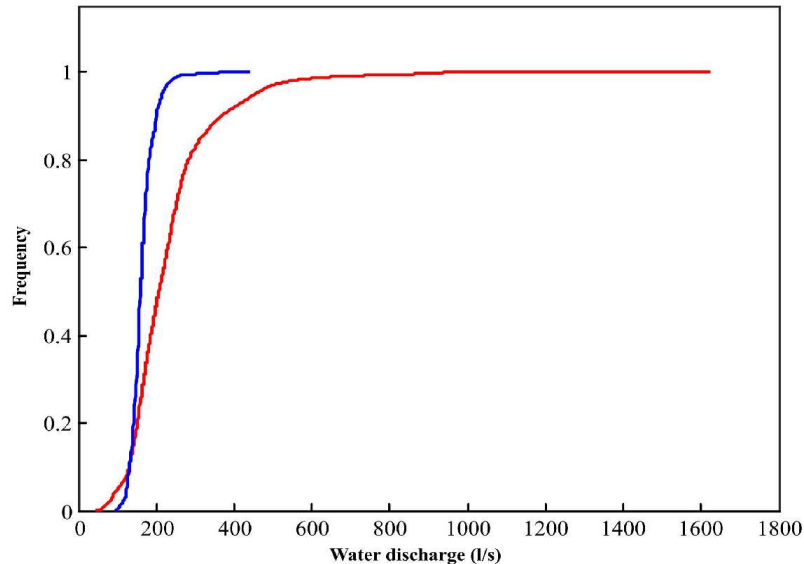


Figure 17. Hydraulic regime of the Hammerbach between 1995 and 2005 (a) and from 2006 to 2008 (b). All values represent an average of the water discharge per month. The red indicates the highest monthly average value over the sampling period, the blue indicates the total average values, and the yellow signifies the lowest monthly average.

Even though the number of years sampled in Figure 17.b is less than in Figure 17.a (11 years against 3 years), a new trend is clearly visible in the Hammerbach behavior. The former monthly extreme values (in red) higher than  $200 \text{ ls}^{-1}$  have disappeared after 2005 and the total average values (in blue) in (17.b) are lower than in (17.a).

Figure 18 shows the same trend with 80% of the Hammerbach discharge below  $182 \text{ l s}^{-1}$  after 2006 in opposite to the value around  $283 \text{ l s}^{-1}$  before. Regrettably, few Schmelzbach data are available in the same period (one month of data with two flood events was recorded during the field campaign of December 2009), but these data seem to confirm the prior observations.



*Figure 18. Cumulative frequencies against water discharge for Hammerbach between 1995 and 2005 (red curve) and 2006 from 2008 (blue curve).*

#### 4.4 Potential hypothesis and explanations of the new hydrological behavior

Five different hypotheses potentially explain this phenomenon:

- (i) - the high flood of August 2005 has probably caused the plugging of sinkholes with sediments or tree lump or plugged a former active conduit in the Hammerbach network.
- (ii) - the dredging of the riverbed between the sewage plant and the entrance of Lurgrotte Semriach (including the Lurbach dam) in summer 2006 may have destroyed one or more infiltration sinkholes (see Figure 19 a&b).
- (iii) - the new behavior of the Lurbach is due to a change in weather conditions.
- (iv) - a lack of relevant data could make a misinterpretation of the system (few Lurbach and Schmelzbach data are available between 1995 and 2009).
- (v) - a combination of two or more upper hypotheses could explain the complexity to understand the cause of the new behavior.

With regard to the prior data analysis, several answers may be provided for the five assumptions:

- (i) - the presence of a delayed flood peak of  $792,5 \text{ l s}^{-1}$  the 26 August 2005 at 23:30, is in disagreement with the assumption that a high flood which plugged the main Hammerbach conduit. That does not mean that the Hammerbach conduit is not plugged but that the two floods cannot be the only reason for the changed behavior of the Hammerbach. The plugging may become progressively greater in time due to slow accumulation of sediments.
- (ii) - this assumption could really explain the new behavior, because dredging boulders were installed overall the Lurbach banks to prevent against river-edge erosion during Lurbach floods. These rocks could also prevent a diffuse infiltration of the stream into the limestone layer. Nevertheless, the presence of the sinkhole before the Lurbach dam (Figure 19.c) shows that a part of the sinkholes are still active, in spite of the fact that no other sinkholes were seen in the Lurbach banks during the investigations of July 2010.

- (iii) - in the precipitation data at our disposal, no significant changes in the weather condition is visible after August 2005.
- (iv) - a time set of Schmelzbach/Lurbach discharge correlated with Hammerbach discharge could confirm or falsify the hypothesis of a new behavior with a major part of the Lurbach water flowing directly to the main conduit of the Lurgrotte.
- (v) - as the Lurbach system is a complex and still not sufficiently investigated system, the assumption (v) seems to be the most realistic to explain the new Lurbach behavior.



**Figure 19. Dredging/cleaning work of the Lurbach banks/riverbed and Lurbach dam in 2006 (a&b) compared with the present situation in July 2010. An active sinkhole is visible in the left hand side in (c). © Photos: H. Kusch(a&b)**

Figure 19 shows the Lurbach riverbed between the sewage plant of Semriach and the dam. The photos a. and b. show the Lurbach dredging in summer 2006 which could potentially cause the destruction of sinkholes. The photo c. was taken in July 2010 and shows clearly an active sinkhole before the dam.

To answer these questions, further investigation is needed for having a better understanding of the global behavior of the Lurbach catchment. A new field campaign could be made in a greater time span (for example between six and twelve months) with one or more tracers experiments, and with new point of interest for example, a new investigation point in the Tanneben massif and Eichberg sinkholes. Another idea will be to try to see if the Badlgraben creek is really not connected with the Lurgrotte under high water conditions (important caves are present along the Badlgraben stream).

## 4. Modeling with MODFLOW:

Prior to modeling, one basic hypothesis with respect the hydrology of the Lurbach system (for more details see the previous part) is made: only the **Tanneben massif** (surface of 8,3 km<sup>2</sup>, see Figure below) is modeled with MODFLOW, because the upper part of the Lurbach catchment flows on an **impermeable schist layer** and thus provides an **allogenic recharge** to the lower karstified part.

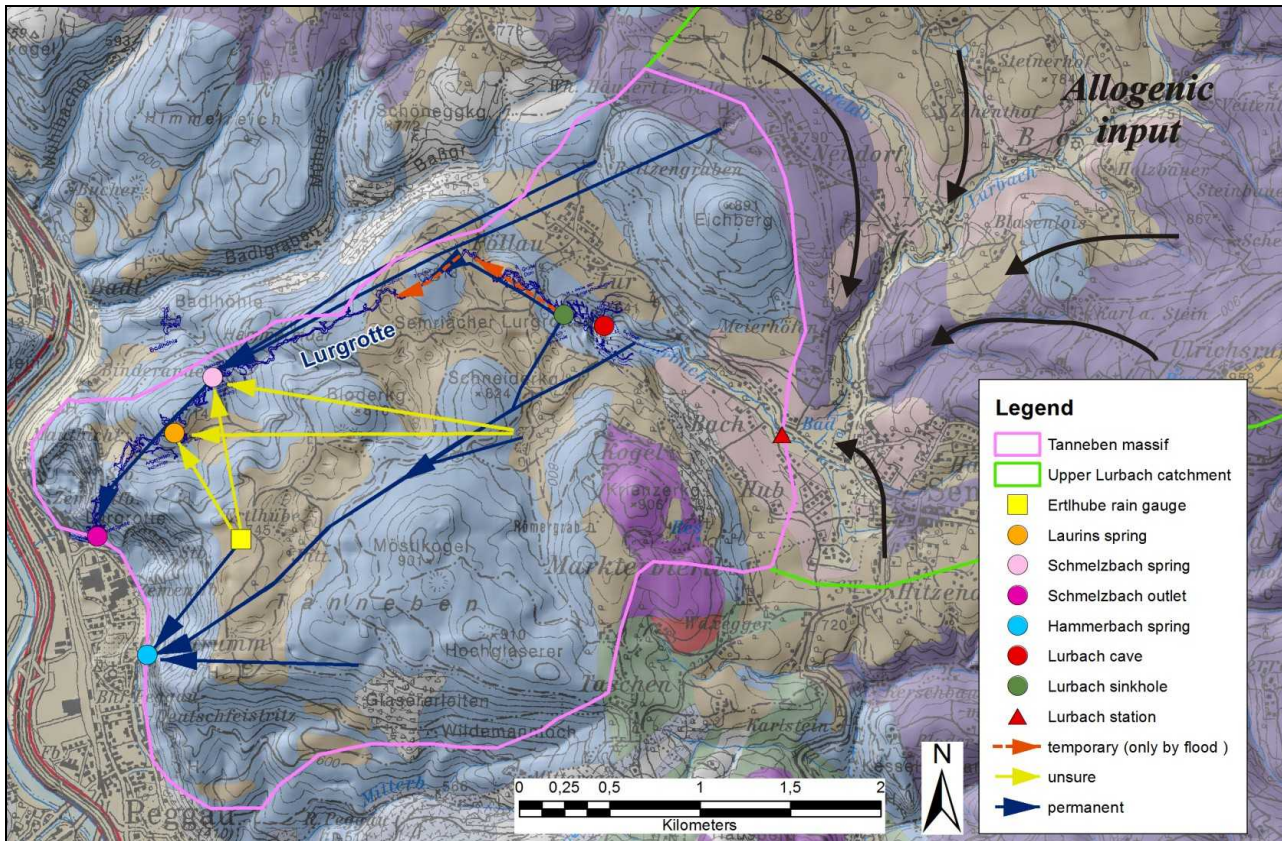


Figure 20. Map of the Tanneben massif (pink line) with the measurement network and the flowing directions of the Lurbach system (redraw after Oswald 2009).

This means that the input can be divided in two categories:

- one defined as the **recharge** (precipitation-evapotranspiration) and given within the entire Tanneben plateau: **the autogenic input**.
- the other defined as upper Lurbach water discharge and given as localized input at some particular points of the catchment, the so-called Lurbach sinkholes located after the Lurbach station and the Lurgrotte. This is the **allogenic input**.

### 4.1 Model design

All models were built with three or four layers.

#### 4.1.1 Three-layer model

**Two three-layer models were built** with a grid of 69\*48 cells and a mesh size of 100 m by 100 m. A no-flow boundary condition was defined for each layer along the boundaries of the Tanneben catchment. Two constant head cells were fixed over the model thickness at the locations of the Hammerbach spring and Schmelzbach outlet (Figure 24).

The Tanneben topography was taken as model surface and defined with the raster data of the area using the software Arc-GIS. In order to have an altitude in the grid corresponding to the mesh size of the model (the size of the cells in Arc-GIS was 10 by 10 m, whereas the models cells are 100 by 100 m), the data were adapted with the help of Matlab (Figure 21).

The first layer was defined as the upper layer of the model with a thickness from the land surface to 400 m asl. (which is the altitude of Peggau, the base level of the catchment).

The thickness of each of the two underlying layers (second, third) was set to five meters.

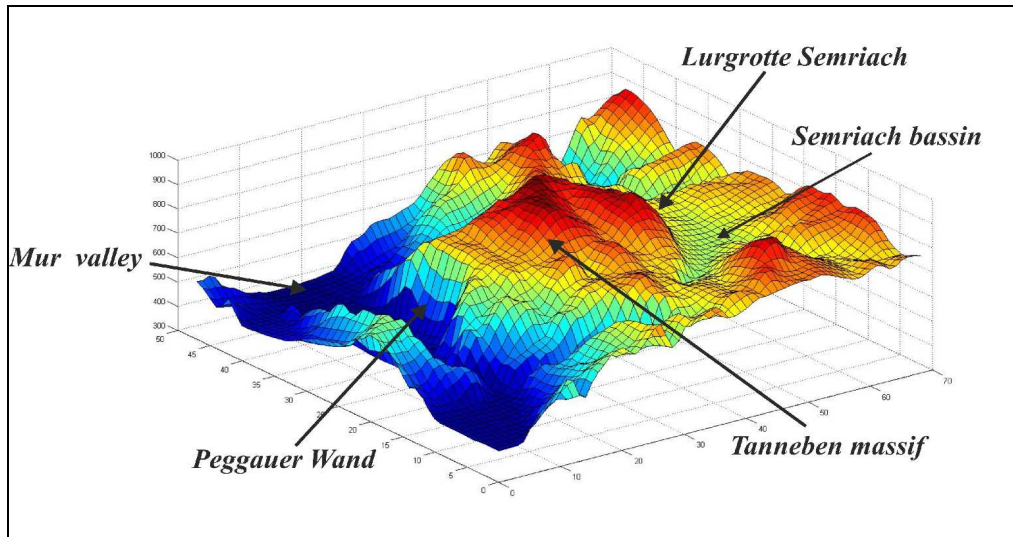


*Figure 21 Topography of the area under investigation calculated with the Arc GIS raster data using Matlab.*

The geometry of the models was defined for taking into account the flow particularities of the Tanneben catchment as showed in Figure 20.

In **Model 1**, the first layer was defined as an **unconfined** limestone matrix with a low horizontal hydraulic conductivity (see Figure 22). In the underlying layers, cells with higher hydraulic conductivity were embedded in the same low-conductivity matrix to represent karst conduits. The second layer was set as **confined-unconfined** and included a large conduit with a high horizontal hydraulic conductivity, which represents the Lurgrotte, and a conduit with a lower horizontal hydraulic conductivity for the Hammerbach network. The connection between the Lurgrotte and the Hammerbach received a lower K value in order to create a constriction effect (and thus to attempt to reproduce the Hammerbach threshold effect).

The third layer was defined as **confined-unconfined** with a conduit for the Hammerbach and a little conduit simulating the Laurins spring.

In the layers two and three, the hydraulic conductivity of the limestone matrix was set to higher values in the upper part of the Tanneben catchment than in the rest of the area, in order to simulate the high sinkhole density of the Eichberg hill.

The vertical hydraulic conductivity was set to  $10^{-4} \text{ ms}^{-1}$  everywhere in the model, except the two points which should receive the allogenic input of the upper Lurbach catchment (at the entrance of the Lurgrotte and the Hammerbach conduit), where it was given a value of  $10 \text{ ms}^{-1}$  over the entire model thickness.

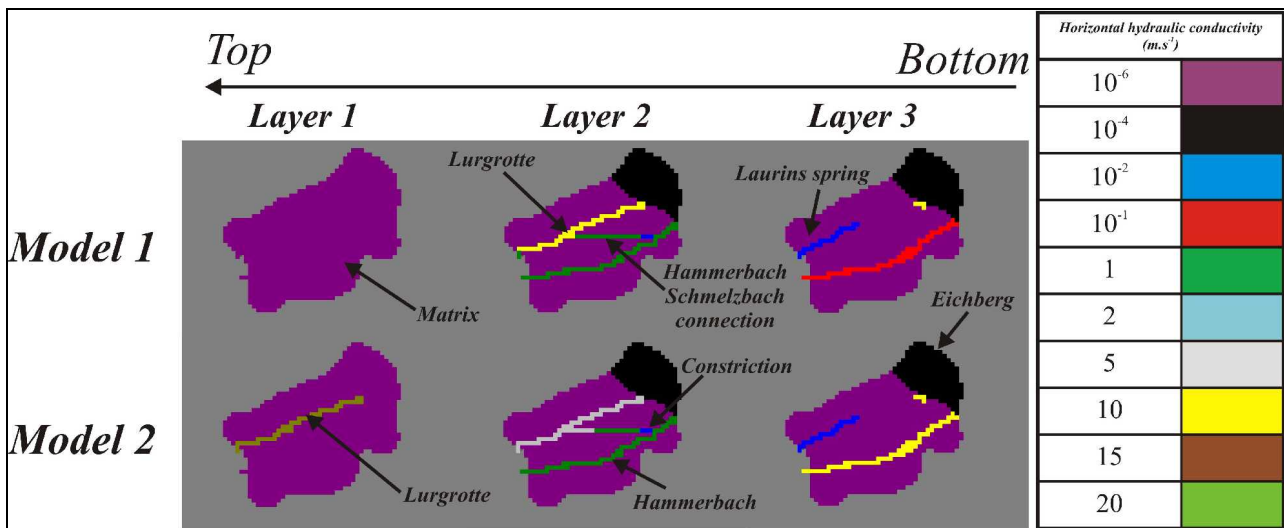


Figure 22. Comparison of the geometry of both three-layer models.

**Model 2** was built on different assumptions than those of Model 1 (see Figure above). The Lurgrotte was included in the first **unconfined** layer and received a very high horizontal hydraulic conductivity. This conduit is expected to be active at high floods.

In layer two, the geometry is identical to that of Model 1, but with a lower horizontal hydraulic conductivity for the Schmelzbach conduit. This intends to allow an important drainage at normal hydrological conditions. The layer three is identical to that of Model 1 but received a higher conductivity for the Hammerbach conduit. The layers two and three were set as **confined-unconfined**.

The Eichberg area is defined similar to the Model 1.

The values of the vertical hydraulic conductivity were identical to those of Model 1.

#### 4.1.2 Four-layer model

The four-layer models were built with a grid of 46\*43 cells and a mesh size of 100 m by 100 m. The boundary conditions were identical to those of the three-layer models. The topography was identical to that of the three-layer model but with a supplementary layer at the bottom.

The geometry of the four-layer models was built on the same assumptions as the three-layer models, but the possibilities to create more complex drainage systems are enhanced by the supplementary fourth layer.

In all cases presented in Figure 23, the first layer was defined as an **unconfined** homogeneous limestone matrix extending from the land surface to 385 m asl.

The second layer was identical in all models and included a large conduit, representing the Lurgrotte, embedded in a limestone matrix with a low horizontal hydraulic conductivity. A limestone matrix sub-region with higher horizontal hydraulic conductivity was implemented in the Northern part of the catchment to represent the highly karstified Eichberg hill. The second layer received a constant thickness of 5 m and was set **confined-unconfined**. In the model named "**Model Ideal Geometry**", the Lurgrotte conduit received a higher K-value than in the other models.

The third and fourth layers included both limestone matrix and karstic conduits.

In the **Model 1**, the third layer included two connected conduits, which supply the Schmelzbach outlet and the Hammerbach spring, respectively. The hydraulic conductivity of these conduits was

lower than that of the conduits in the second and fourth layer. The fourth layer was defined with a Hammerbach conduit draining the South side of the Tanneben catchment and a conduit representing the Laurins spring on the North side. The layers three and four were 5 and 10 m thick, respectively.

The third layer in **Model 2** was almost identical to that of Model 1, but the connection between Hammerbach and Schmelzbach received a lower horizontal hydraulic conductivity for simulating a constriction effect. The K value of the Hammerbach is also higher than in the Model 1. Thus, it is expected that the third layer of Model 2 drains more water than that of Model 1.

The last layer is divided in two parts representing two different areas of the Tanneben catchment: one for the Hammerbach and the other for the Laurins spring, the latter of which received a higher hydraulic conductivity of the matrix limestone to allow more drainage. The layers three and four were 5 and 10 m thick, respectively.

The third layer of the “**Model ideal geometry**” received a conduit with a different geometry which begins after the Lurbach station and divides in two sub-conduits. One is directly connected to the Hammerbach spring, the other to the Schmelzbach outlet. A tributary conduit was created in the south part of Tanneben to take into account some famous caves such as the Wildemannloch, which can store water in the Tanneben massif (Figures 20 and 23).

The fourth layer combines a low limestone matrix and Eichberg matrix with a Laurins spring conduit more developed than in the former models and a new assumption for the Hammerbach drainage network. These hypotheses are based on the fact that the Lurbach infiltrates before his entrance into the cave (in the Lurbach sinkhole) but also after his entrance in the Lurgrotte (in the so-called Lurbach disappearance) and supplies water only to Hammerbach. The layers three and four were 5 and 10 m thick, respectively.

In all models, layers three and four were defined as **confined-unconfined**.

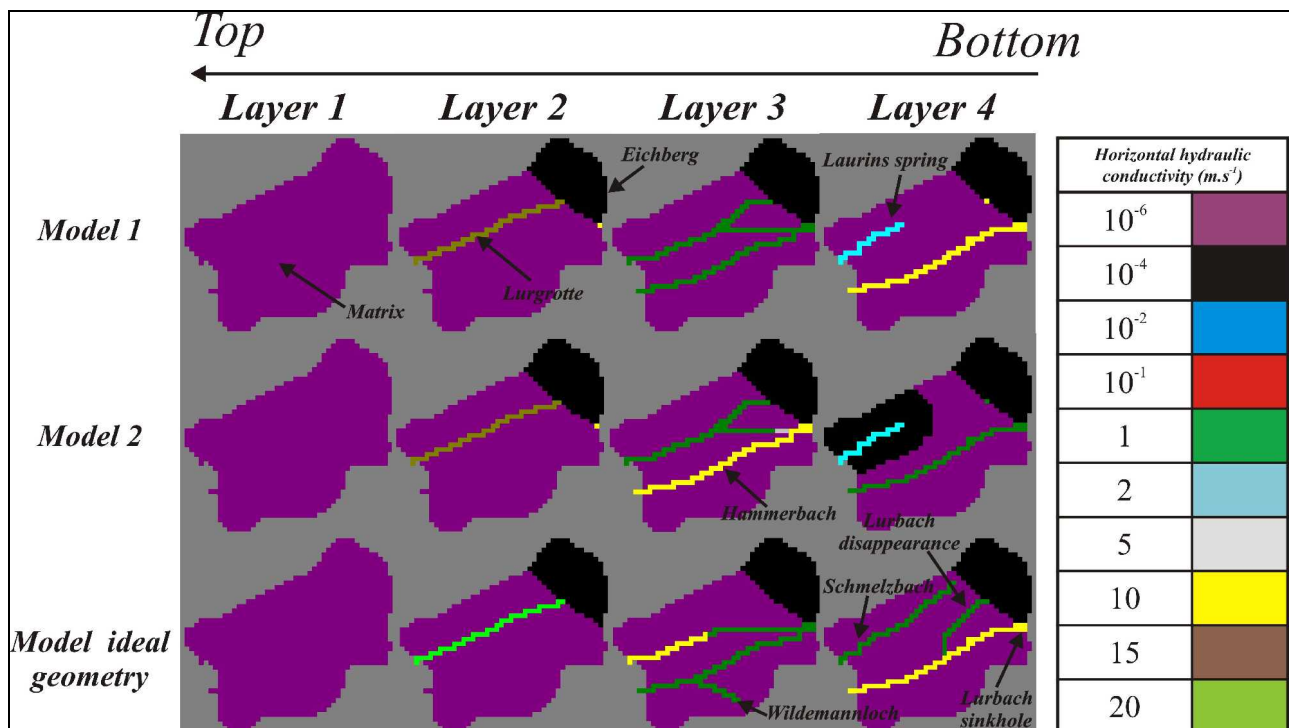


Figure 23. Comparison geometry of the four-layer models.

If we consider the hydrological behavior of the system (see the previous chapter) and the flow directions presented in Figure 20, the four layer models seems more realistic as the three layer models because it takes into account more different features of the conduit network. In the four layer models, the model named “**Model ideal geometry**” appears to be the most realistic model of the aquifer geometry.

All of these models were initially tested in steady state to have a first evaluation of their relevance.

## 4.2 Steady state

Two water discharge sub-regions were also added on the Hammerbach spring and Schmelzbach outlet for monitoring the output water discharge. The solver used for the modeling was the DE-45 solver.

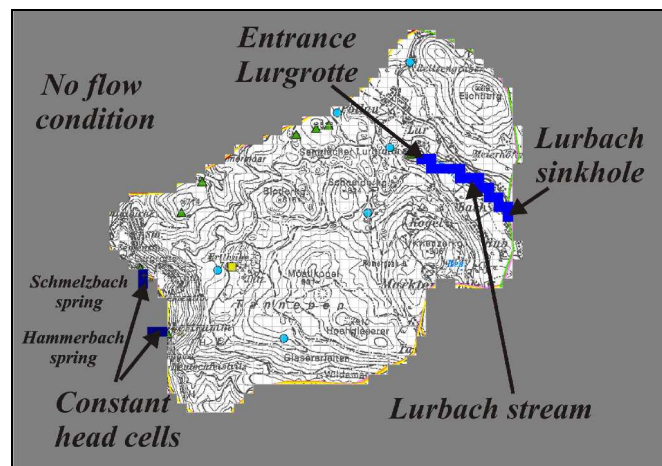


Figure 24. Boundary condition in steady state for the three and four-layer models.

### Calibration attempt with discharge data of the Steirische Beiträge

In this part, we attempted to reproduce the behavior of the Lurbach system described by Behrens et al., (Steirische Beiträge zur Hydrogeologie, 1992). The discharge data were already presented in the previous chapter (Tab.1).

#### 4.2.1 Input data

For approaching the real climatic conditions over the year, an evapo-transpiration rate and a precipitation rate were calculated. They are based of the meteorological data of the rain gauge of Semriach (located at 720 m. asl) over **a period of nine years (1971-1980)**.

The temperature was calculated based on a linear correlation between the surrounding weather stations of Graz, Frohnleiten and Teichalpe (which is located in the North of the region of interest at 1.180 m asl). This is a compromise between the different altitudes of the catchment where highly different temperatures can be measured at the same time.

The mean precipitation rate over the period is roughly of **897 mm.y<sup>-1</sup>**.

The mean evapo-transpiration rate was determined with the **Turc equation** (D.M. Gray, 1970) as:

$$ET_r = \frac{P}{(0,9 + [\frac{P}{(300 + 25T + 0,05T^3)}]^2)^{0,5}}$$

where P is the mean annual precipitation rate.  
T is the mean annual air temperature (°C) take as 7,4

yielding 445 mm.y<sup>-1</sup>.

The recharge is deduced from the difference between the precipitation value and the evapo-transpiration:

$$R = P - E_{tr}$$

Event	Annual mean	Wettest year	Driest year
Rainfall (mm.y <sup>-1</sup> )	897	1.351	669
Evaporation (mm.y <sup>-1</sup> )	445	476	410
Recharge (mm.y <sup>-1</sup> )	451	874	259

Tab.3: Precipitation, evapo-transpiration and recharge data on the Tanneben massif for the period 1971 1980.

The calculated recharge rate was used as input for the MODFLOW **Recharge package**. The localized allogenic input was simulated using the **Well package** in MODFLOW, i.e. **injection wells** were used to represent the Lurbach input. The total injection rate was distributed to the model layers, and a high vertical hydraulic conductivity was assigned to the concerned cells. This allows to simulate the sinkholes and vertical shafts where the Lurbach loses water. In each model, the Well package was essentially used for two cells: at entrance of the Lurgrotte and after the Lurbach station.

The values of the allogenic input data were the Lurbach discharge data, taken from Behrens et al., (1992) (see Tab.4).

	Lurbach discharge input (ls <sup>-1</sup> )	Well input (ls <sup>-1</sup> )	Recharge input (ms <sup>-1</sup> )
<b>Event</b>	Three-layer models		
<b>Normal</b>	141	191,7	1,43 10 <sup>-8</sup>
<b>Flood</b>	15.300	12.001	2,77 10 <sup>-8</sup>
<b>Drought</b>	4	4,3	8,21 10 <sup>-9</sup>
	Four-layer models		
<b>Normal</b>	141	184	1,43 10 <sup>-8</sup>
<b>Flood</b>	15.300	12.448	2,77 10 <sup>-8</sup>
<b>Drought</b>	4	4	8,21 10 <sup>-9</sup>

Tab.4: Lurbach data compared to Well and Recharge input data for the three and four-layer models.

In order to respect the homogeneity of the MODFLOW unities, all recharge rate and injection rates were given to MODFLOW after a conversion in ms<sup>-1</sup> and m<sup>3</sup>s<sup>-1</sup>.

## 4.2.2 Modeling results

### Three-layer models

Table 4 presents the modeling results for the two three-layer models. As we can see, the results look very similar in drought events. Under flood conditions, Model 2 show a discharge of the Hammerbach spring too high due to the high conductivity of the cells supplying the spring. These trend is also observable at normal conditions. This indicates that there is an influence of the hydraulic conductivity of the conduit cells on the distribution of flow to the two springs.

	<b>Model 1</b>		<b>Field data</b>	
<b>Discharge (ls<sup>-1</sup>)</b>	Schmelzbach	Hammerbach	Schmelzbach	Hammerbach
<b>Drought</b>	49,9	38,4	15,4	33
<b>Flood</b>	10.277	2.007,3	11.400	2.000
<b>Mean discharge</b>	129,9	208	82,7	193
	<b>Model 2</b>		<b>Field data</b>	
<b>Drought</b>	46,9	41,3	15,4	33
<b>Flood</b>	10.042,8	2.214,3	11.400	2.000
<b>Mean discharge</b>	104,5	233,4	82,7	193

*Tab.5: Schmelzbach and Hammerbach water discharge in steady state for the three layer models with the same input values compared to measured values from Behrens et al, (1992).*

If we compare these results to the values from Behrens et al., (1992) we can see that the two models drain more water during drought period than the real system. This might be explain by the fact that the recharge input for the drought period overestimates the real recharge during a drought. The value was taken during the driest year over the sampled period, but in reality the recharge might be zero during a long-lasting drought.

In case of flood events, the modeled discharge is in good agreement with the data, except in the Model 2 for the Hammerbach, where slightly more water is drained in the model than observed. For the mean annual discharge, the two models give reasonable results, but the lower Schmelzbach discharge of Model 2 is more realistic.

In Model 2 the Schmelzbach hydraulic conductivity of the second layer (the Hammerbach and Schmelzbach systems are totally independent in the first and third layers) is lower than in the Model 1. The results seems to indicate that a part of the Schmelzbach water flows to the Hammerbach system. This is in contradiction to the assumptions of Behrens et al. (1992), but a recent discussion with a scientist of the Joanneum Research Institute (R. Benischke, personal communication) seems confirm the possibility of this behavior.

In summary, the two steady-state three-layer models reproduce the data from Behrens et al., (1992) reasonably well but the hypotheses on the conduit geometry appear to be less realistic compared to the four-layer models.

### Four-layer models

Table 6 presents the spring discharges of the four-layer models in steady state compared to the data from Behrens et al., (1992).

As seen in the three-layer models, the behavior of all models at severe drought is similar and predict higher discharge at the Schmelzbach outlet than the data. As discussed above, this can potentially be explain by the autogenic recharge input data, which probably over-estimates the infiltration during drought conditions.

	<b>Model 1</b>		<b>Field data</b>	
<b>Discharge (ls<sup>-1</sup>)</b>	Schmelzbach	Hammerbach	Schmelzbach	Hammerbach
<b>Drought</b>	42,1	49,4	15,4	33
<b>Flood</b>	9.975,7	2.764,5	11.400	2.000
<b>Mean discharge</b>	103,3	233,6	82,7	193
	<b>Model 2</b>		<b>Field data</b>	
<b>Drought</b>	45,7	45,8	15,4	33
<b>Flood</b>	10.119	2.621,1	11.400	2.000
<b>Mean discharge</b>	125,1	211,7	82,7	193
	<b>Model ideal geometry</b>		<b>Field data</b>	
<b>Drought</b>	43,2	48,4	15,4	33
<b>Flood</b>	8.676,9	4.066,8	11.400	2.000
<b>Mean discharge</b>	114,4	223	82,7	193

*Tab.6: Schmelzbach and Hammerbach water discharge in steady state for the four-layer models compared to measured values.*

The first two models show good agreement with the data under flood conditions. In contrast, the Hammerbach discharge calculated by the model named “Model Ideal Geometry” is too high. This is due to horizontal hydraulic conductivity of the conduit named Lurbach disappearance, which brings more Schmelzbach water to the Hammerbach spring.

The three models agree well with the mean discharge. The “Model ideal geometry” represents a compromise between the two other models with results between the Model 1 and Model 2.

In spite of the poor match with the flood data, the model named “Model ideal geometry” is considered to be better than Model 1 and Model 2, because it is more strongly based on hydraulic assumptions derived from the field observations and the flowing directions presented in Figure 20.

Thus, the geometry of this model was used for further calibration attempts in steady state. To this end, only the horizontal hydraulic conductivity values were changed. Figure 25 shows the resulting geometrical assumptions: the Lurgrotte connection to Hammerbach received a lower conductivity, while the hydraulic conductivity of connection between Hammerbach and Schmelzbach was increased.

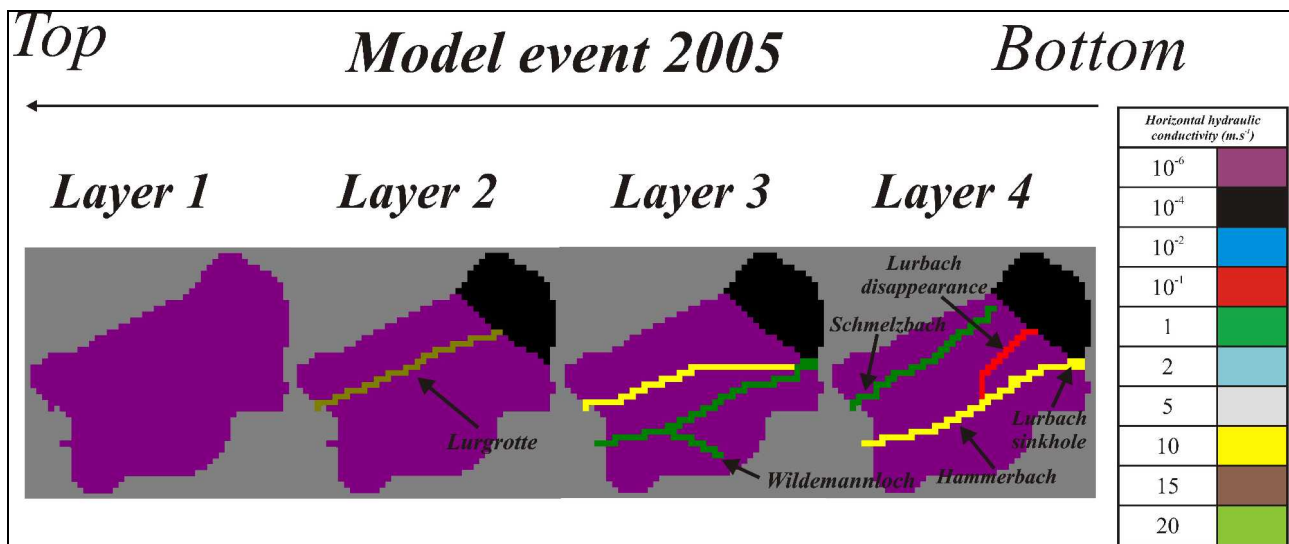


Figure 25. Presentation of the geometry of the Model Event 2005.

The model was named “**Model event 2005**” because it was firstly tested to calibrate the Hammerbach flood of August 2005 (see the previous chapter for a short presentation, and the following for the transient-state calibration) but after that, it was also tested in steady state and gave better results than the three other four-layer models.

Table 7 gives the results of the steady-state simulation. As all other models, the discharge under drought conditions is overestimated. However, the flood event results are better than those of the “Model ideal geometry” and have the advantage to agree with realistic geometrical assumptions. Finally, the mean discharge results are in reasonably good agreement with the data of Behrens et al., although the discharge at the Schmelzbach outlet is higher than in reality.

	Model event 2005		Field data	
	Schmelzbach	Hammerbach	Schmelzbach	Hammerbach
<b>Discharge (ls<sup>-1</sup>)</b>				
<b>Drought</b>	47,8	43,9	15,4	33
<b>Flood</b>	10.571,2	2.172,5	11.400	2.000
<b>Mean discharge</b>	136	201,4	82,7	193

Tab.7: Schmelzbach and Hammerbach water discharge in steady state for the Model event 2005 compared to measured values..

To conclude with the steady-state modeling, we can claim that further investigation is recommended in transient state, because the steady-state modeling is only based on punctual data of different events, which have different intensity, time scale and frequency. Moreover, the flow in the real karst aquifer is certainly not steady state, in particular, under mean and flood conditions.

In case of the drought event, the overestimation probably comes from the initial hypothesis. The recharge value was derived from the recharge during the driest year of the monitored period. This is considered a **rough approximation** only, but no other data were available.

These data can be also criticized because they represent only extreme events: no Lurbach discharge more than 1 m<sup>3</sup>s<sup>-1</sup> and no Hammerbach upper 1,6 m<sup>3</sup>s<sup>-1</sup> were present in the data set as disposal. Finally, the data of Behrens et al. (1992) need to be evaluated with care because they might have high measurement errors, particularly the discharge measured at Lurbach station during droughts and high floods.

### 4.3 Transient State

After testing in steady state, the different models were also tested under transient conditions.

#### 4.3.1 Initial conditions

In all cases, the initial water table was computed in steady state and used as initial condition for the transient simulation. All models were computed with the MODFLOW solver DE-45.

#### 4.3.2 Hypothetical master recession curves by Behrens et al. (1992)

The first attempt was to reproduce the Hammerbach and Schmelzbach recession behavior described by Behrens et al., (1992). In their assessment, Hammerbach and Schmelzbach recession are computed over a period of 200 days combining results of several events. In their hypothesis, the catchment does not receive recharge during this period. It is nevertheless precised, that the longest period without recharge during the investigation was **35 days** and the rest of the time was extrapolated (Behrens et al, 1992).

#### Three-layer model

The calibration was firstly tested with the three-layer models. The water table was simulated with the allogenic and autogenic input data used for the normal (mean) hydrological steady-state conditions.

The transient simulation requires two additional hydraulic parameters for the modeling: the **specific yield** and the **specific storage**.

The **specific yield** corresponds to the **drainage porosity** and is used for the flow calculation by MODFLOW only if the computed layer is **unconfined**. In all models, we have decided to attribute the same specific yield values of 0,01 for the matrix and 0,001 for the conduits. Since only layer one is unconfined and does not incorporate conduit cells, the latter value does not have any effect on the simulation results.

The **specific storage** is used for the flow calculation by MODFLOW only if the layer is **confined** (which happens to be the case for all layers except for layer one).

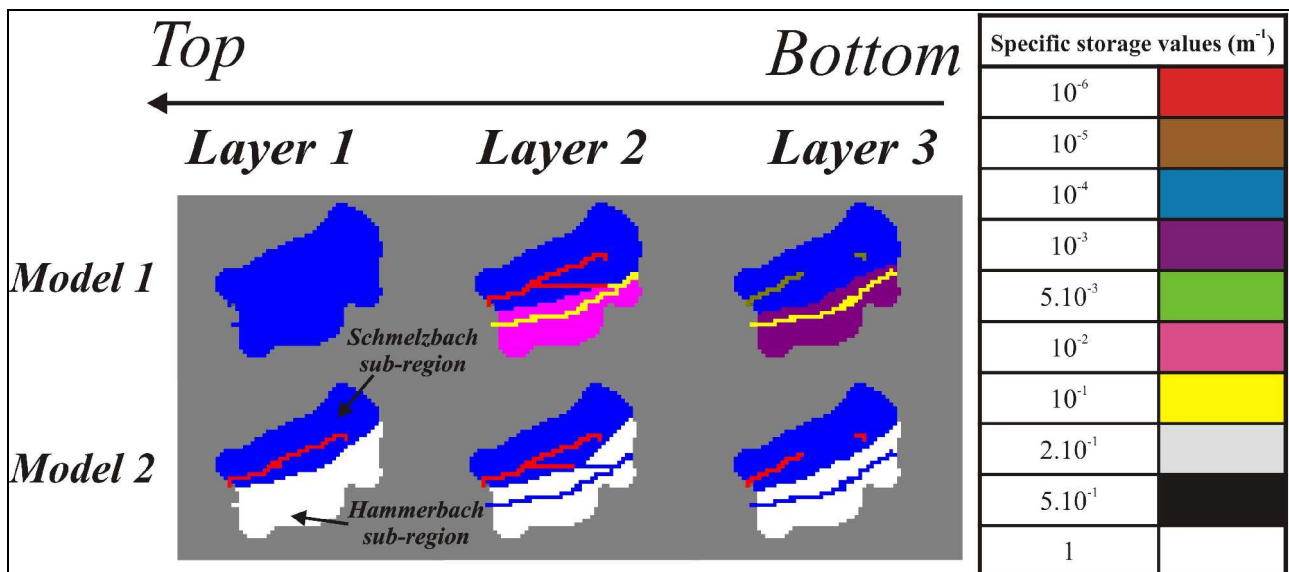
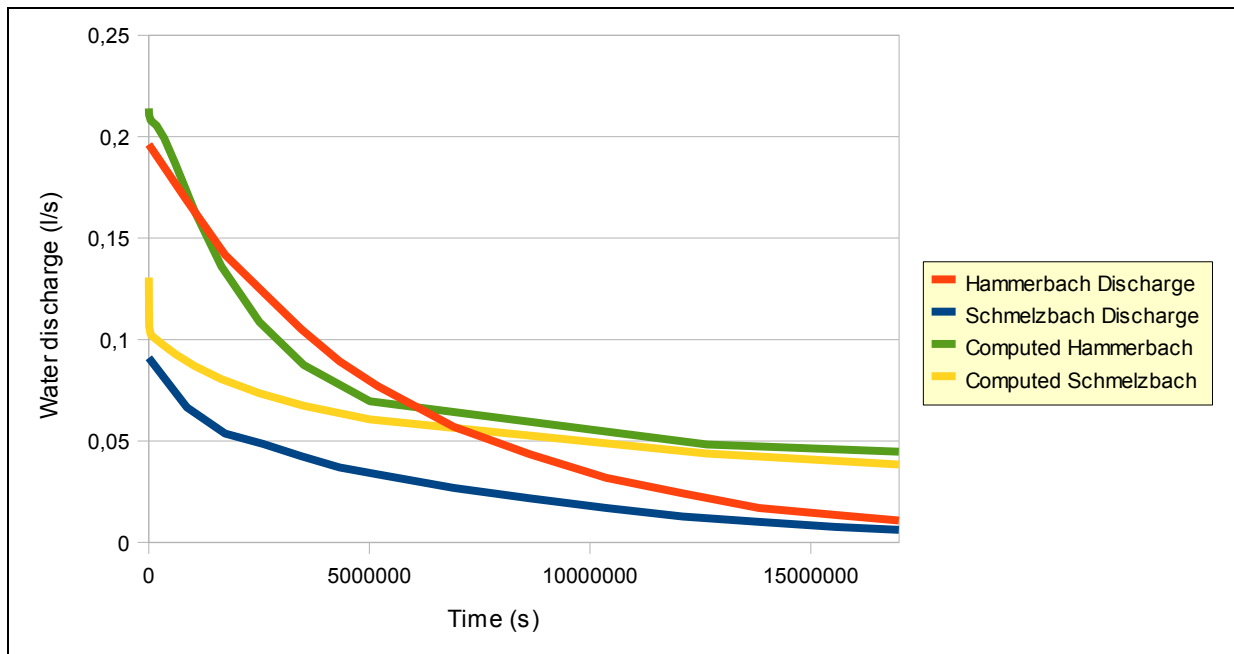


Figure 26. Comparison between the specific storage used for the three-layer model 1 and Model 2.

In the case of the modeling of the curve of Behrens et al., the specific storage was defined with the assumption to make two different drainage areas in the Tanneben massif, in order to reproduce the two different recession behavior of the Schmelzbach and Hammerbach stream.

Figure 26 presents the specific storage values for the Model 1 and 2. In Model 1, the first layer was defined with a constant low storage value in order to allow a rapid infiltration through the Tanneben limestone. The layers two and three were divided in two area with a lower specific storage value in the vicinity of the Schmelzbach area. The value of Hammerbach conduits was set higher than the Hammerbach matrix value, in order to force a delayed flow to the Hammerbach spring (this is conceptually totally false, but it was only to see the influence of the storage over the conduit behavior).

In Model 2, the specific storage was defined identically for all layers with the same sub-regions and values. The Schmelzbach matrix value was lower as the Hammerbach matrix value. This assumption was also applied to the conduits where the Schmelzbach and Laurins spring conduits receive low storage value as the Hammerbach conduits.



**Figure 27. Calibration attempt for the three-layer Model 1. The red and blue curve are taken from Behrens et al., whereas the green and yellow are the recession curve computed with the Model 2. The modeling time represents approx. 200 days.**

Figure 27 presents the recession curve of the Schmelzbach and Hammerbach for Model 1 compared to the curves of Behrens et al. The Model 1 clearly shows a different drainage behavior and indicates that in the model the Tanneben massif drains water more slowly than in reality.

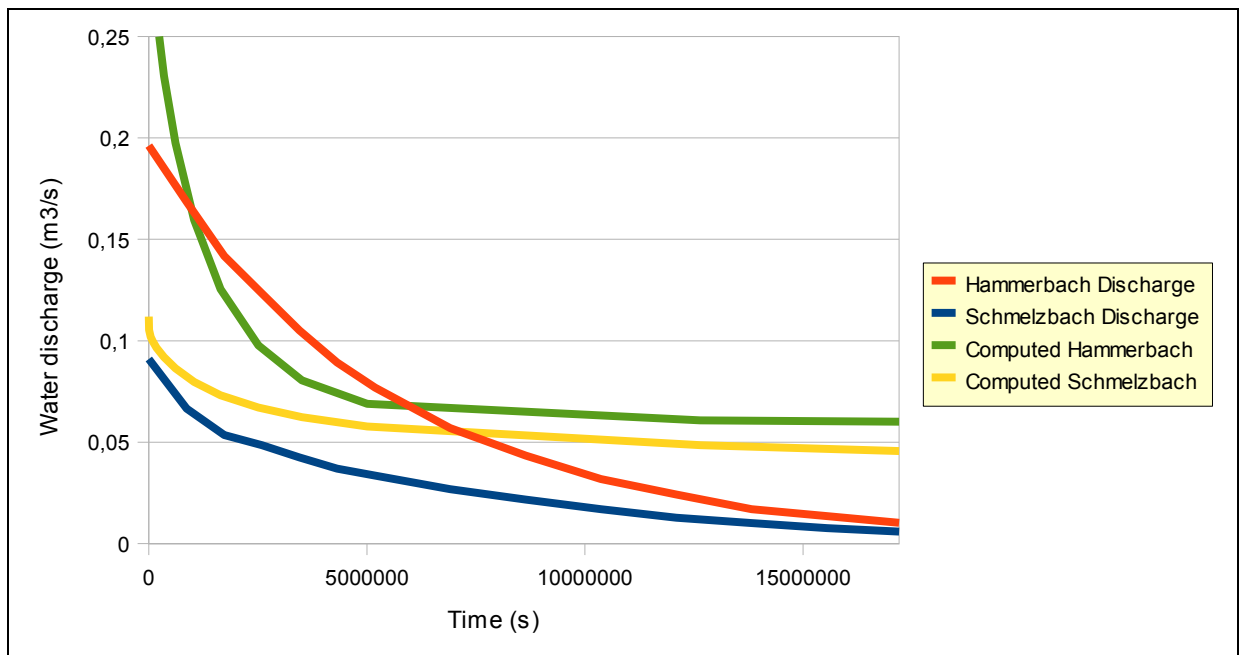


**Figure 28.** Calibration attempt for the three-layer Model 2. The red and blue curve are taken from Behrens et al., whereas the green and yellow are the recession curve computed with the Model 2. The modeling time represents approx. 200 days.

Figure 28 shows a calibration attempt for Model 2. As we can see here, the calibration is worse than that for Model 1. The computed Hammerbach discharge is initially too high and decreases too fast. The specific storage assumptions for the Model 2 give poor results.

In either case, the recession behavior computed does not agree with the curves proposed by Behrens et al., (1992). Model 1 provides better results because the convergence of the two curves is reached at a lower discharge than in Model 2, which fits better to the curves by Behrens et al. Nevertheless, the storage geometry seems totally unrealistic.

#### Four-layer models

The initial conditions and the specific yield in the four-layer models were identical to those of the three-layer models.

For the specific storage, the general assumptions were different as the three-layer models (Figure 29). After an homogenous first layer with a low specific storage value, which should allow a rapid infiltration to the vadose zone, two sub-regions were defined in the Tanneben massif:

- one where the matrix should retain more water to allow a slow drainage to the Hammerbach spring.
- the other where the matrix releases the water more rapidly to supply the Schmelzbach outlet.

This corresponds to the observation that the recession curve of the Hammerbach decreases more slowly than that of the Schmelzbach.

The value of the Hammerbach conduits was also set higher than the matrix value.

The same values of specific storage were used in case of Model 1 and Model 2 and could allow a comparison of the influence of the horizontal hydraulic conductivity.

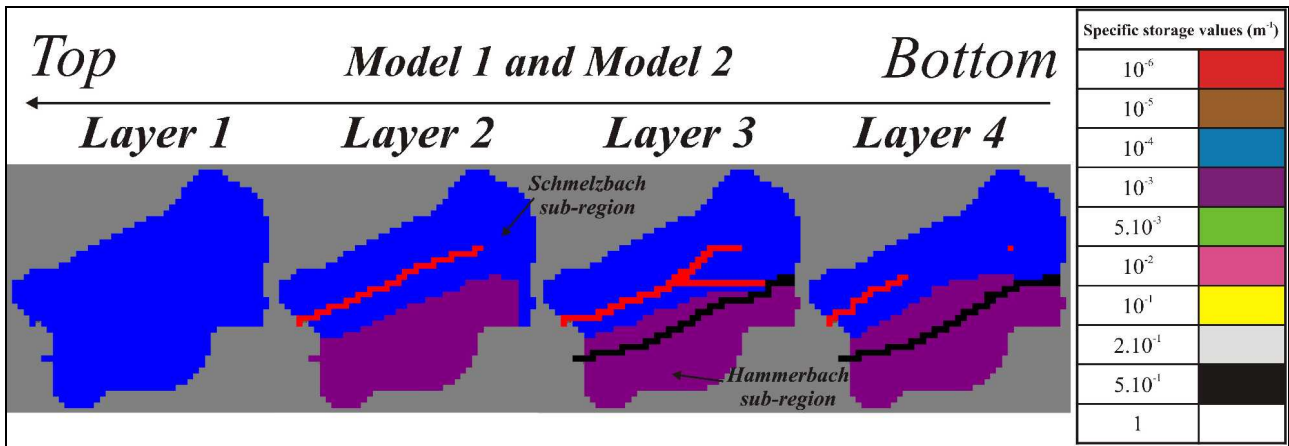


Figure 29. Specific storage used for the Model 1 and 2.

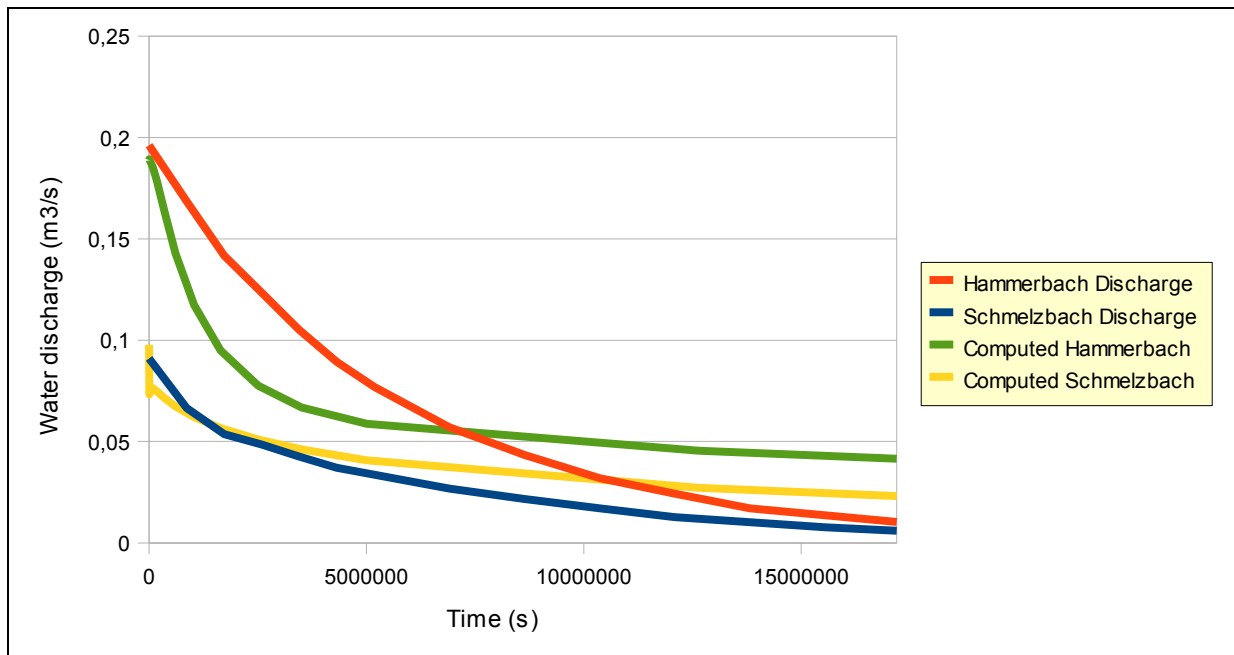


Figure 30. Calibration attempt for the four-layer Model 1. The red and blue curve are taken from Behrens et al., whereas the green and yellow are the recession curve computed with the Model 1. The modeling time represents approx. 200 days.

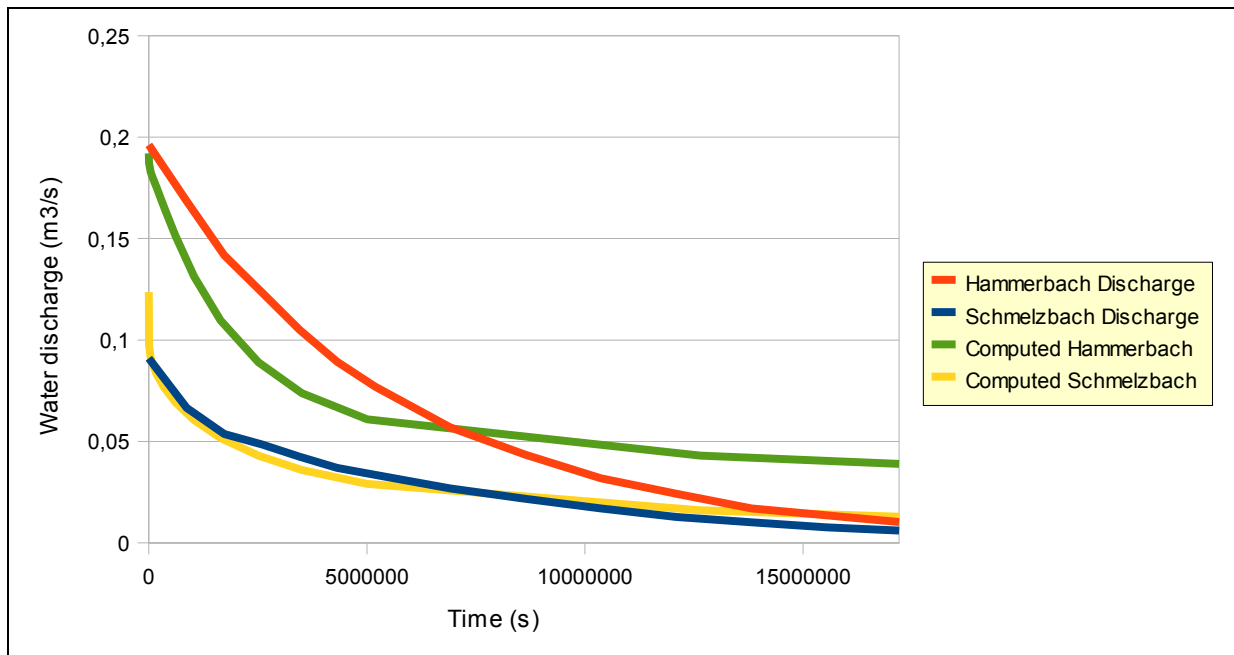
Figure 30 presents the recession behavior of the Lurbach system with the four-layer Model 1. The computed Schmelzbach discharge is closer the Schmelzbach data than that of the previous three-layer models. Nevertheless, the convergence of the Hammerbach and Schmelzbach discharge, which was reached in the three models layers, is not obtained here. The Hammerbach curve also shows a recession behavior clearly different from the curve by Behrens et al.

Figure 31 presents the modeling results of the Model 2. Here the Schmelzbach behavior is reproduced well, in spite of the fact that the Schmelzbach discharge was too high at the beginning of the simulation (which is due to the initial condition). The Hammerbach recession still does not match the curve of Behrens et al., but appears to be better than the three prior curves.

As the specific storage was the same for the Model 1 and Model 2, the results of the figures 30 and 31 can be explain by the different hydraulic conductivity geometries:

- the Model 2 has a constricted connection between the Hammerbach and Schmelzbach which has prevent a flow of water from the Hammerbach network to the Schmelzbach network.

- the lowest layer of the Model 2 present a sub-region around the Laurins spring with a high hydraulic matrix conductivity: this can potentially explain the difference of drainage with the Model 1.



**Figure 31.** Calibration attempt for the four-layer Model 2. The red and blue curve are taken from Behrens et al., whereas the green and yellow are the recession curve computed with the Model 2. The modeling time represents approx. 200 days.

To conclude this part, the attempt to reproduce the recession behavior of the data present in Behrens et al, was not fully successful but we can formulated some conclusions, criticisms and suggestions:

- it is very challenging to calibrate springs which are interconnected.
- the hypothetical curves in Behrens et al., are a combination of several different measured curves and not a one event curve. **A recession period of 200 days** (like the time span of the curve) over the Lurbach and Tanneben catchment **seems unrealistic**, and was (and will) probably never been observed.
- the hypothetical recession seems to be too slow. In reality, the Hammerbach and Schmelzbach can reach discharge values lower than  $30 \text{ l s}^{-1}$  in summer within time periods much shorter than 200 days. Thus, the calibration might be more successful if the data is taken from specific recharge events.
- the two curves from Behrens et al., give no information about the recession behavior of the Lurbach system during hydrological events such as summer (karst) flash floods.
- the assumptions of the specific storage values (Figures 26 and 29) in the Hammerbach conduits are probably false for the four-layer models and for the first three-layer model.

In summary, the (partial) failure of the attempt to calibrate the models to the curves by Behrens et al. (1992) does not seem to be a serious problem, because the hypothetical curves appear to do not adequately represent the recession behavior of the Lurbach system.

### 4.3.3 Flood of August 2005

After trying to reproduce the behavior of the Lurbach system with the hypothetical recession curve from Behrens et al., it was attempted to reproduce the big flood of August 2005 (described Figure 16 in Chapter 3) with our models.

This event is of particular importance because the assumptions of the new behavior of the system were implemented with it.

A brief description of the event before the modeling is necessary: the flood begins on 20/08/2005 at 12:15 with a Hammerbach discharge of 198,7 ls<sup>-1</sup>. The maximum discharge is reached on 21/08/2005 at 20:15 and amounts to 1.623,1 ls<sup>-1</sup>. Then, the discharge decreases very fast to a value of 339,2 ls<sup>-1</sup> on 26/08/2005 at 13:00. After that, a second flood happened but with a slow intensity and a maximum discharge of 792,5 ls<sup>-1</sup> on 26/08/2005 at 23:30. Finally, the discharge decreased slowly over a period of six month (127 ls<sup>-1</sup> on 14/02/2005 at 3:00).

This event can be denominated under the appellation of “Karst Flash flood” because it had a high intensity during a small period of time.

The event was simulated with the four-layer model named “**Model event 2005**”, which is an improvement of the model named “**Model ideal geometry**” presented previously. The initial water table was computed with input data taken from an artificial event in order to have a simulated water discharge at the Hammerbach spring equal to the flood peak. The Schmelzbach discharge was not computed because no Schmelzbach data were available for the same period. The solver DE-45 was used here.

The little peak of 792,5 ls<sup>-1</sup> should be also simulated. It was firstly computed separately in order to find the required input data which provide the same water discharge. These data were given as input data to the model in the 7 time step of our simulation.

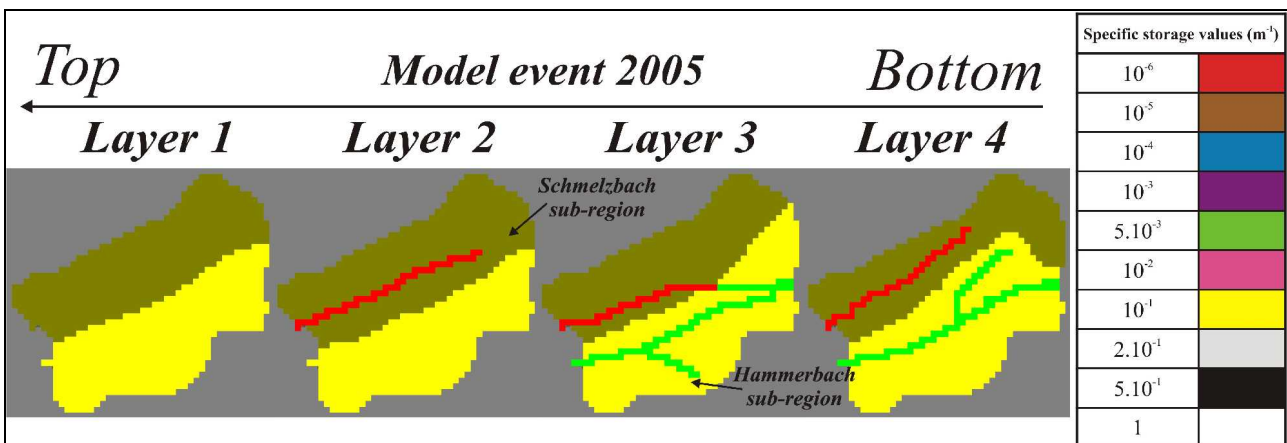
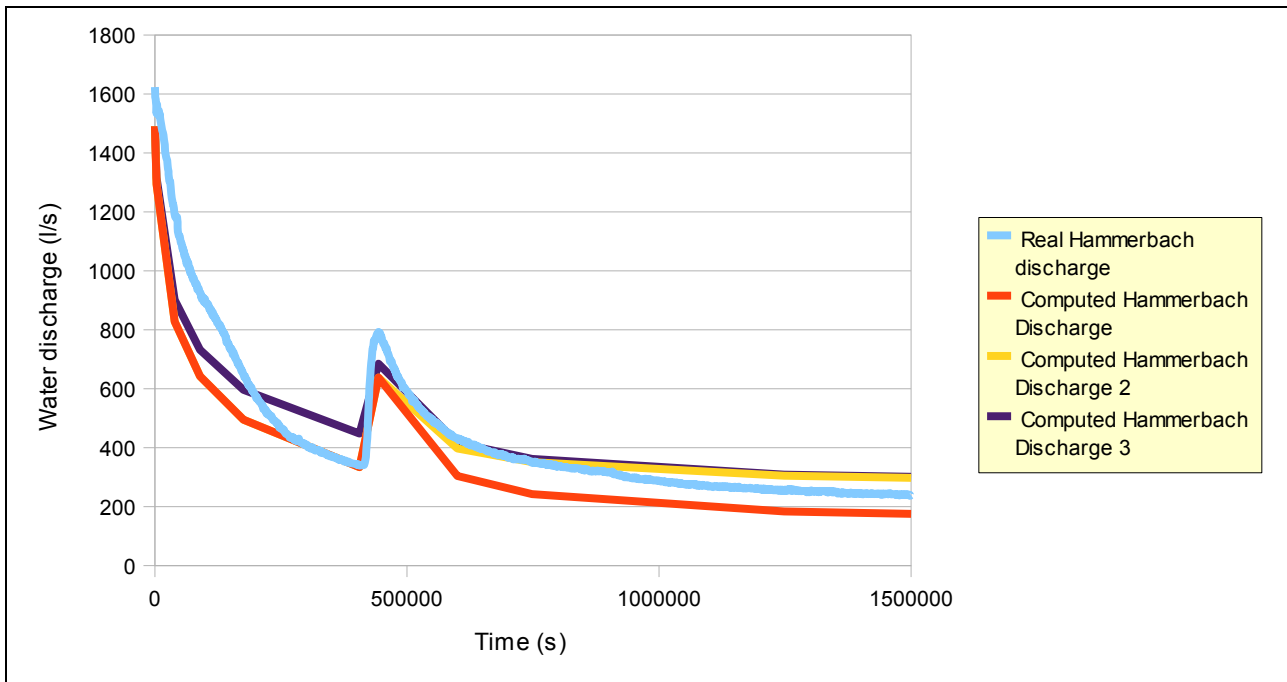


Figure 32. Specific storage used for the “Model event 2005”.

A new specific storage geometry was defined with assumptions in better agreement with the reality. As the former models, the Tanneben was cut in two sub-regions, but in this case the specific storage value of the Hammerbach conduits was lower than the surrounding matrix.



*Figure 33. Calibration attempt of the Hammerbach data of August to December 2005. The blue curve is the sampled curve. The yellow, red and purple curve are the modeling curves with input data.*

Figure 33 shows the results of the simulations: all curves were simulated with the same conduit and matrix geometry the same specific yield and storage. The only change was from the input data given during the event.

The red curve receive only new input for simulating the little flood peak, whereas the purple receive a constant recharge over the event. The yellow curve receive a constant recharge before the event.

The yellow and purple curve show a good agreement with the measured data in spite of the lower discharge at the start of the simulation, which is followed by a period with higher discharge before the second little event for the purple curve.

This modeling can receive some criticisms:

- because of the lack of Schmelzbach data, only the behavior of the Hammerbach was computed. No attention was given to the behavior of the Schmelzbach outlet. This is a rough assumption because the Hammerbach and Schmelzbach drainage areas are interconnected during high floods such this one.
- the initial water table was made with an artificial event (that means that we have only tried to have a water discharge at the outlet which correspond to the maximum water discharge of the event).

#### **4.3.4 Events of the field campaign of December 2008**

The next attempt was to calibrate the model to the data of a field campaign, which was carried out between November and December 2008 (Oswald et al., 2009) and aimed to realize a tracer experiment for better understanding of the conduit network.

In this experiment, the data of the Schmelzbach, Hammerbach, Lurbach station and Lurbach cave station were sampled (Figure 34). Precipitation and temperature data of the Ertlhuber rain gauge were also available.

However, only two events have sufficient data to be exploitable in this sampling period.

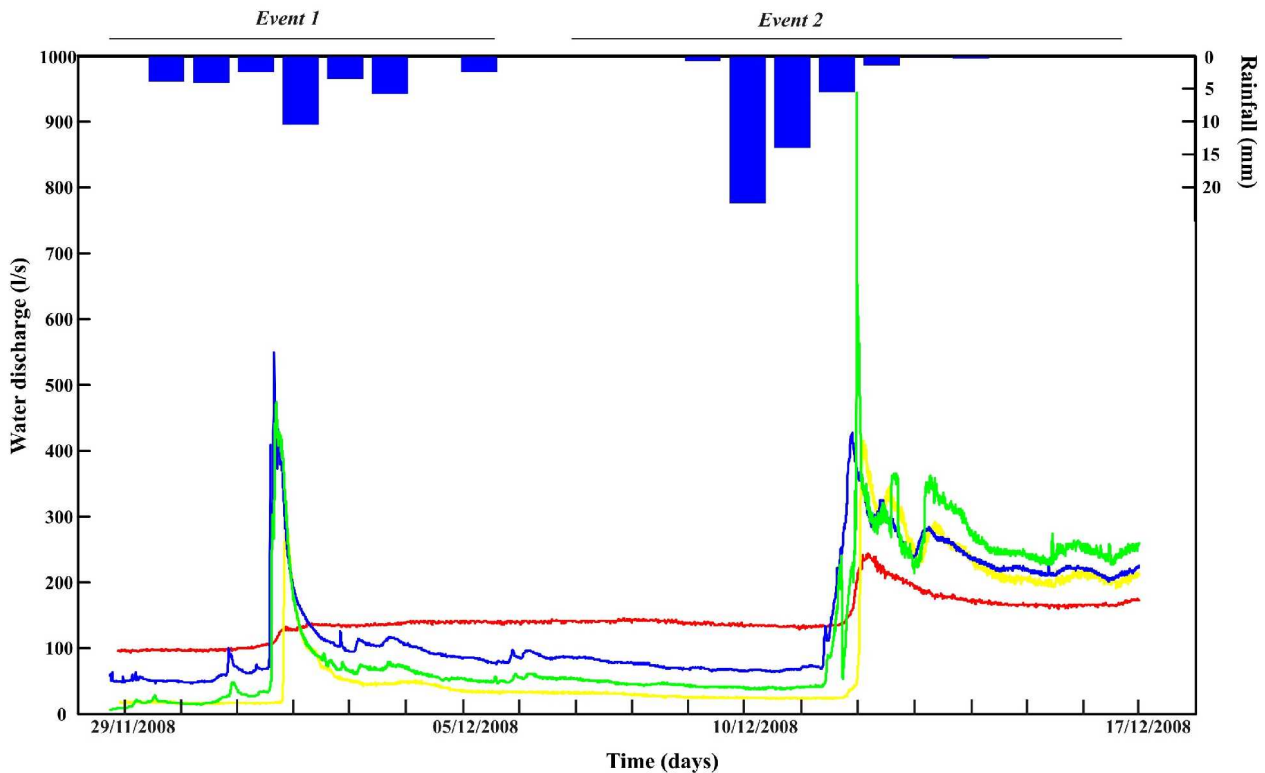


**Figure 34.** Water discharge and precipitation recorded between the 29.11.2008 and the 17.12.2008. The red line represents the Hammerbach discharge, the yellow the Schmelzbach discharge, the green the discharge measured at Lurbach cave station and the blue the discharge at Lurbach station.

This data set is the only case where all input data were available in sufficient quantity to simulate the **allogenic recharge** from the upper Lurbach catchment and the **autogenic recharge** through the Tanneben massif.

The model geometry used here was similar to the geometry of the “Model event 2005” but with some little modifications for the conduit named “Lurbach disappearance,” which received a higher horizontal hydraulic conductivity, and for the connection Hammerbach-Schmelzbach, which was set to  $K = 1 \text{ ms}^{-1}$ .

The specific storage used was the same than the “Model event 2005” (Figure 32).

In each case, the initial water table was computed with an artificial event giving a computed water discharge equal to the measured water discharge. The mean of the precipitation during the event was used as recharge, i.e. evaporation was assumed to be negligible because the temperature was still around  $0 \text{ }^{\circ}\text{C}$  during the experiment.

The first event was simulated from the **28/11/2009 at 17:55** to the **08/12/2008 23:59**.

In the first event, the autogenic recharge rate was given in  $\text{ms}^{-1}$  and the allogenic recharge rate was given in  $\text{ls}^{-1}$  at two different points: the entrance of the Lurgrotte and near the Lurbach station, for simulating the infiltrations sinkholes.

Figure 35 presents the modeling results of the first event. The deep sky blue and brown curve are the results with a constant allogenic input of  $80 \text{ ls}^{-1}$  given to the Lurbach sinkhole, whereas the green and yellow curve are the modeling result of the simulation with an input of  $50 \text{ ls}^{-1}$  to the sinkholes.

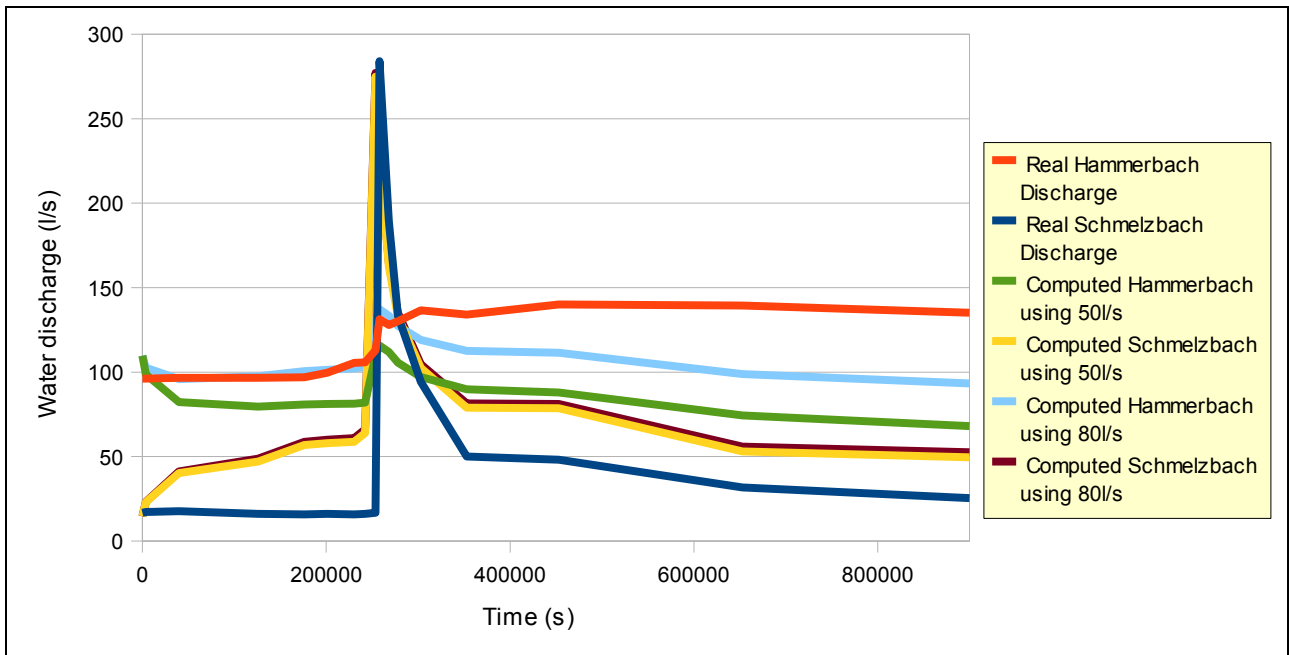


Figure 35. Calibration attempt of the first event.

In spite of the better fit that provide the modeling with  $80 \text{ l/s}^{-1}$  to the Hammerbach curve, this value of  $80 \text{ l/s}^{-1}$  seems to high to agree with the reality.

The input value of  $50 \text{ l/s}^{-1}$  is also a bit high (comparative to the field data of Oswald where a sink of about  $40 \text{ l/s}^{-1}$  between Lurbach station and Lurbach cave station is visible before the event) but is more realistic than the value of  $80 \text{ l/s}^{-1}$ .

The second event was simulated from the **09/12/2008 at 00:00** to the **15/12/2008 at 22:40** . The allogenic input given to the sinkhole was  $80 \text{ l/s}^{-1}$ .

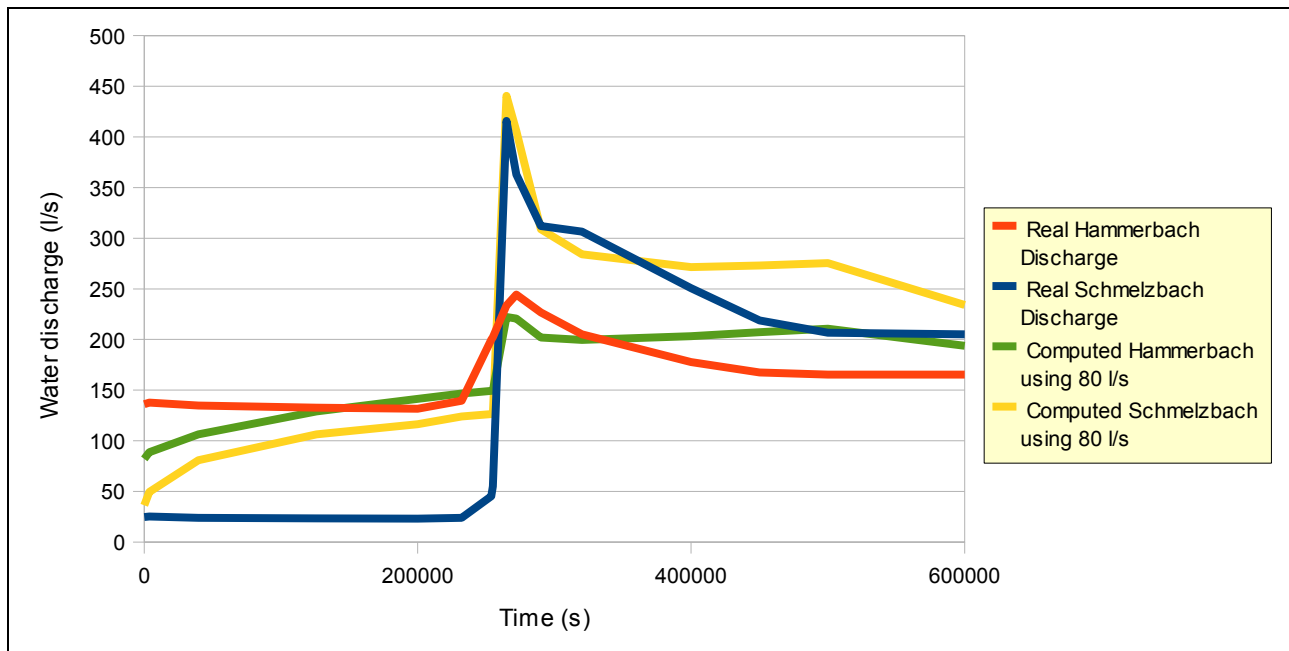


Figure 36. Calibration of the second event.

In this case, the two curves are worst calibrated as the first event because the allogenic input data were problematic. An explication can come from the observation of the two Lurbach curve sampled during the second event.

The discharge sampled at the Lurbach station is lower than the discharge value monitored before the Lurgrotte.

This can be explained by a delay in the Lurbach stream, probably caused by a branch or ice dam rupture (a gap before the flood peak is observable in the Lurbach cave discharge) which give a water pulse into the Lurgrotte.

To conclude this part we can firstly claim that further research will be helpful to have a better understanding of the Lurbach behavior. In spite of a global good fit, the modeling was made with assumptions which over-estimate the volume of water which can infiltrate between the two Lurbach measurement stations. These hypotheses disagree also with the new Lurbach behavior presented on the part 3 of this report.

#### 4.4 Attempt to reproduce the new Lurbach behavior

In order to check if the hypotheses about the new hydrological behavior of the Lurbach system are correct and reproducible with MODFLOW (for more details see the hydrological behavior in the previous chapter), a modified 4 layer model was tested.

The assumptions tested here were the influence on the water discharge of one or several sinkholes/conduits plugged by the big flood of September 2005, or after the dredging of the stream in 2006.

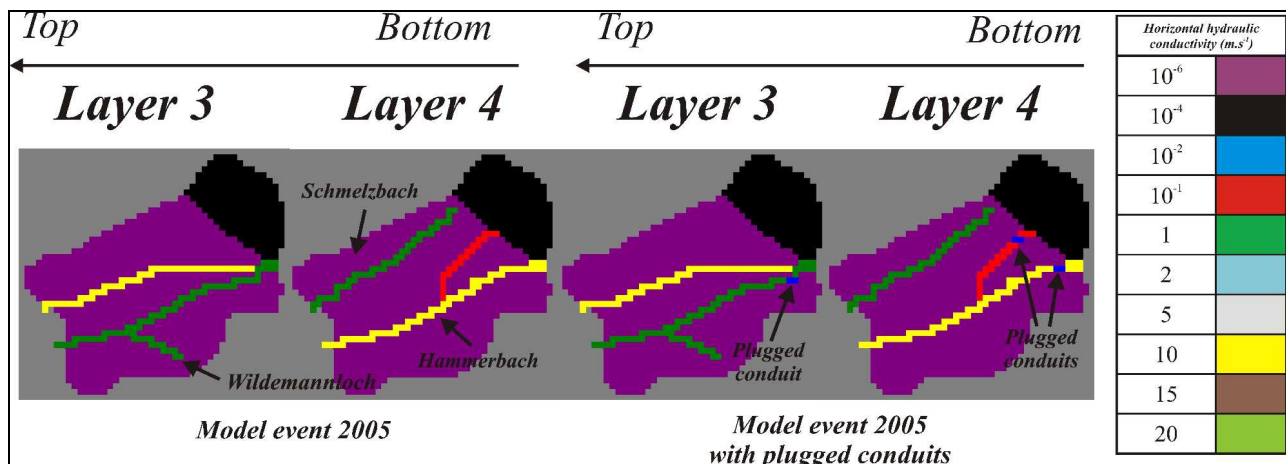
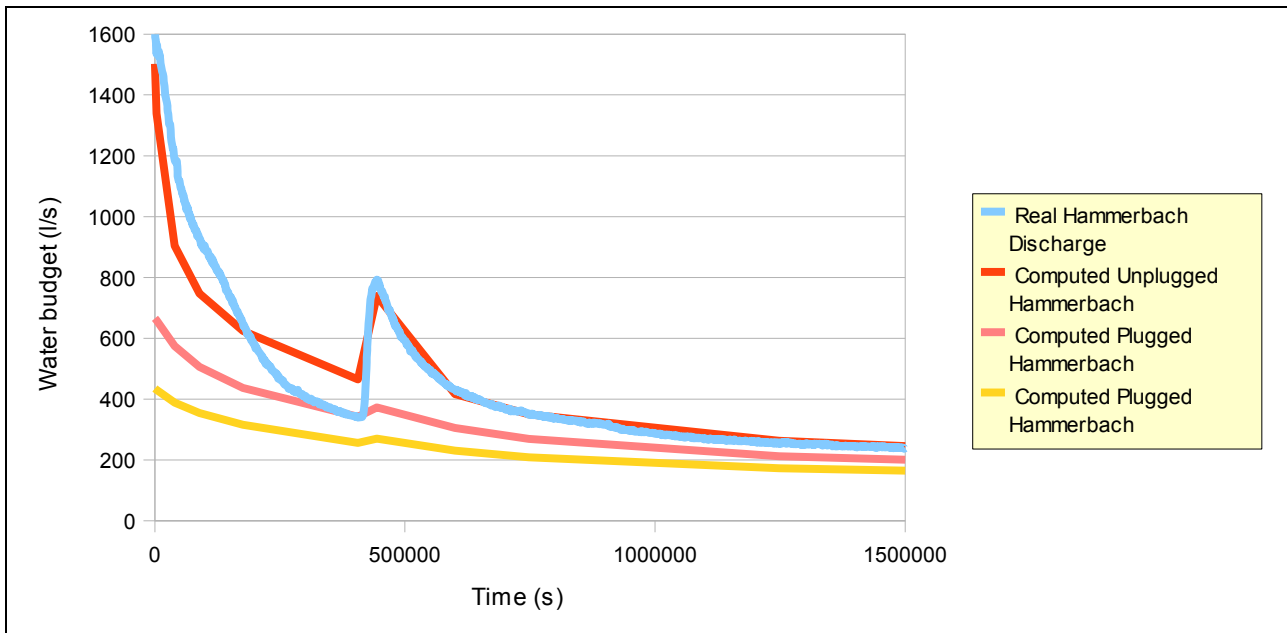


Figure 37. Comparison of the geometry between the Model event 2005 and the Model with plugged conduits.

A four-layer model previously used was employed to reproduce the event of 2005 with a little modification of the hydraulic conductivities of the two first cells (Figure 37) of the Hammerbach conduits in the layer three and four. The hydraulic conductivity was fixed at 10<sup>-6</sup> ms<sup>-1</sup> on the first attempt and 10<sup>-2</sup> ms<sup>-1</sup> for the second attempt instead of 10 and 1 ms<sup>-1</sup> for the third and fourth layer, respectively.

The model was only tested in transient state and used a water table simulated in steady-state with MODFLOW 2000 as initial condition.



**Figure 38. Comparison between the Hammerbach spring discharge of 2005 and the discharge of an event of the same intensity but with a narrowed conduit network.**

Figure 38 presents the results of the modeling of an event of the same intensity than the event of August 2005 but with plugged infiltration sinkholes for the Hammerbach. The blue curve represents the event of August 2005 and the red curve is the simulation of this event.

The pink curve is the computation with plugged sinkhole with a value of  $10^{-2} \text{ ms}^{-1}$  whereas the yellow use a value of  $10^{-6} \text{ ms}^{-1}$ .

The influence of the conductivity of the sinkhole has an important effect on the spring discharge and is coherent with the initial assumptions. Nevertheless, some similar criticisms to those made with respect to the simulation of the event of August 2005 can be made:

- The exclusion of the Schmelzbach from the computation (because no Schmelzbach data are available).

- Some further investigations are necessary, to determinate if the new behavior or the Lurbach system is real or not. A new field data set with Lurbach, Hammerbach and Schmelzbach discharge could be easily answer this question.

## 5. Modeling with MODFLOW-CFP

After modeling of the Tanneben massif in steady/transient state in laminar regime, an attempt with MODFLOW-CFP was made in order to see how the system reacts with turbulent flow (for a presentation of CFP see in the first Chapter).

The previous models were firstly tested with MODFLOW 2000 and CFP in BCF mode but it was found that the iterative solver did not converge.

Thus, simpler models were designed in order to have a correct functioning of MODFLOW-CFP.

The model presented here is a **one layer rectangle model** named “Ultra basic one layer” with **two parallel conduits** connected each other with a sub-conduit located in the center of the model (Figure 39). These two conduits should represent the simplified form of Hammerbach and Schmelzbach streams. The dimensions were from 1400 to 2950 m with conduits cells smaller than the matrix cells. The depth of the layer was fixed constant as 50 m for the matrix and 10 m for the conduits (see Figure 39).

A **constant-head boundary condition** was set only at the East side of the model (where the outlets of the conduits are located).

The initial water table was computed in MODFLOW 96 with the solver DE-45 and an artificial event. The model received autogenic recharge and localized allogenic input directly into the sinkholes entrances. The input into the Hammerbach sinkhole was  $200 \text{ ls}^{-1}$  whereas the Schmelzbach swallow receive  $25 \text{ ls}^{-1}$ . The autogenic recharge was  $2,7 \cdot 10^{-4} \text{ mms}^{-1}$ .

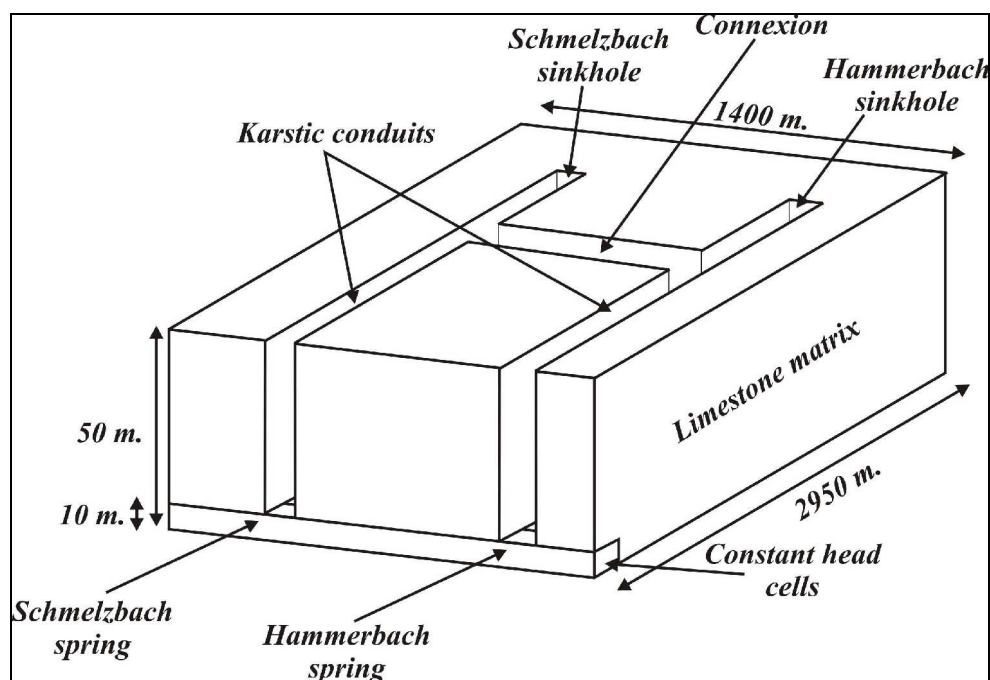
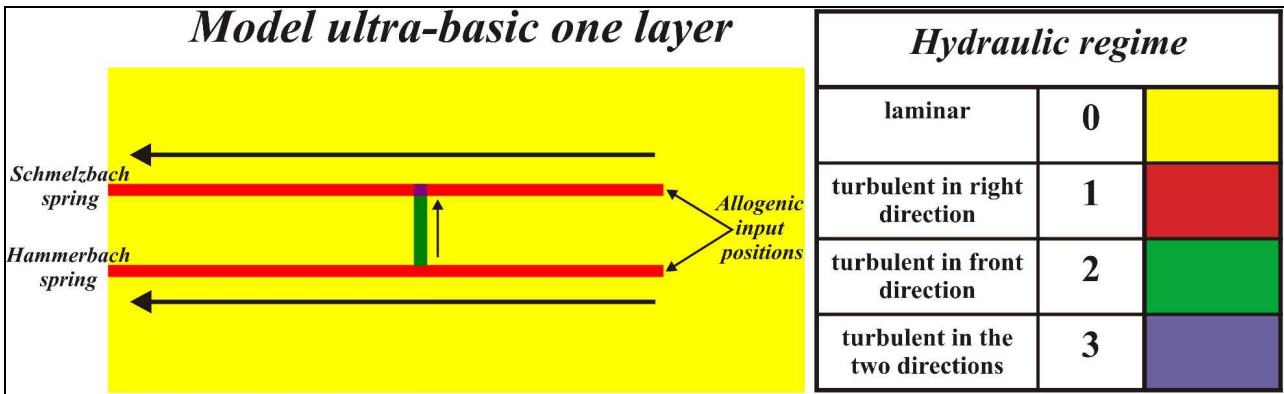


Figure 39. Sketch of the MODFLOW-CFP model.

The occurrence of turbulent flow is presented in Figure 40. As we can see here, Figure 40 reveals a realistic behavior of the turbulent and laminar flow. The laminar flow is only located in the matrix, whereas flow is turbulent only in the conduits and along an appropriate direction (the connection should flow from the Hammerbach network to the Schmelzbach, because the Hammerbach input was higher than the Schmelzbach input).



*Figure 40. Map of the flow of the «Ultra basic one layer» model during the event.*

Figure 41 represents a comparison between the two karstic conduits under the influence of a connection, a constricted connection and two independent conduits. The same input parameters were given for the three computations.

The green and yellow curves represent the Hammerbach spring and Schmelzbach outlet without connection. The red and blue curves are the discharge of Hammerbach and Schmelzbach with a connection with  $K = 10 \text{ ms}^{-1}$  between the two conduits. It is clearly visible that a part of the input Hammerbach water flows through the connection and causes an increase of the discharge of the Schmelzbach spring. Finally, the deep sky blue and purple curves are the Hammerbach and Schmelzbach discharge with a constricted connection with  $K = 1 \text{ ms}^{-1}$ .

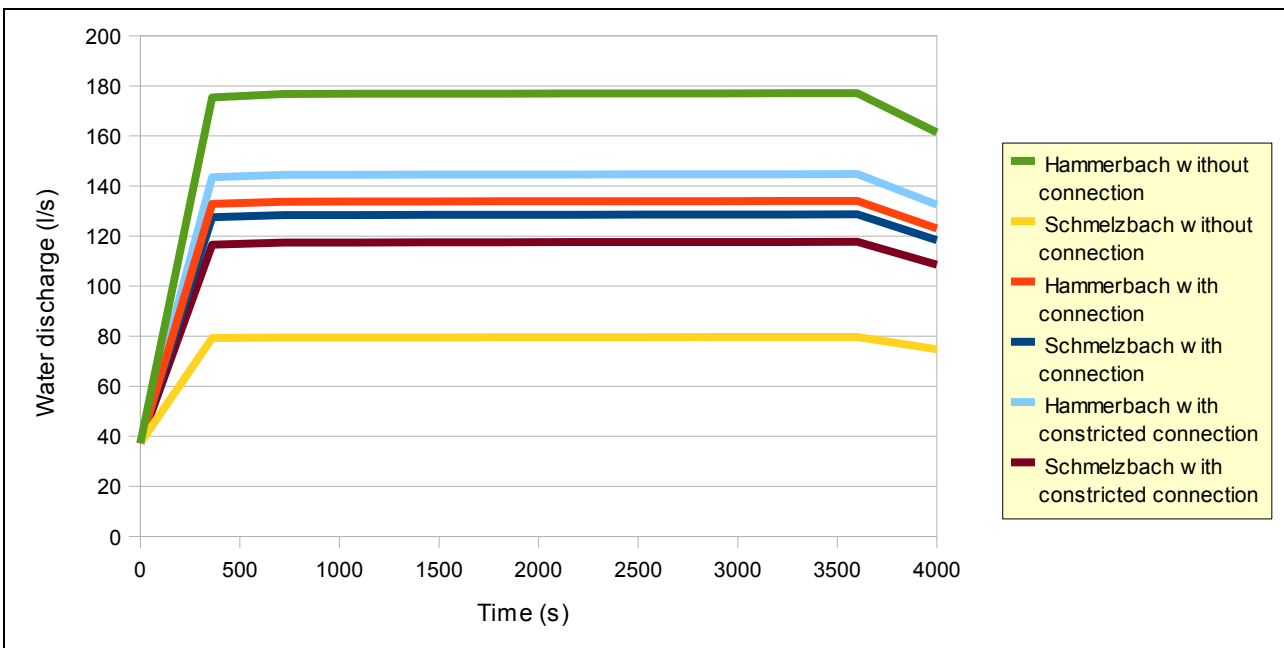


*Figure 41. Comparison between turbulent Hammerbach and Schmelzbach discharge if the model has a connection, no connection or a constricted connection.*

The yellow and green curves are used as reference because their conduits are independent. Their discharge is the sum of the input of their respective sinkholes and the autogenic recharge. The blue and red curves are almost identical because the horizontal hydraulic conductivity of the connection between the two conduits is high ( $10 \text{ ms}^{-1}$ ). The discharge of the Schmelzbach with the constricted connection is lower than the Schmelzbach discharge with the connection with  $K = 10 \text{ ms}^{-1}$ . The constriction thus plays an important role to allow or prevent a massive flow from the Hammerbach network to the Schmelzbach network.

## 6. Comparison between MODFLOW and MODFLOW-CFP

In this part a comparison between MODFLOW and MODFLOW-CFP was realized. The tested model was a one layer model constituted of a conduit embedded in a matrix (Figure 42). The dimensions were from 1500 to 3000 m. The thickness of the layer was 20 m. A constant flow boundary condition was used on the left side of the model, where the conduit outlet is located. The initial conditions were calculated in steady state with an artificial event.

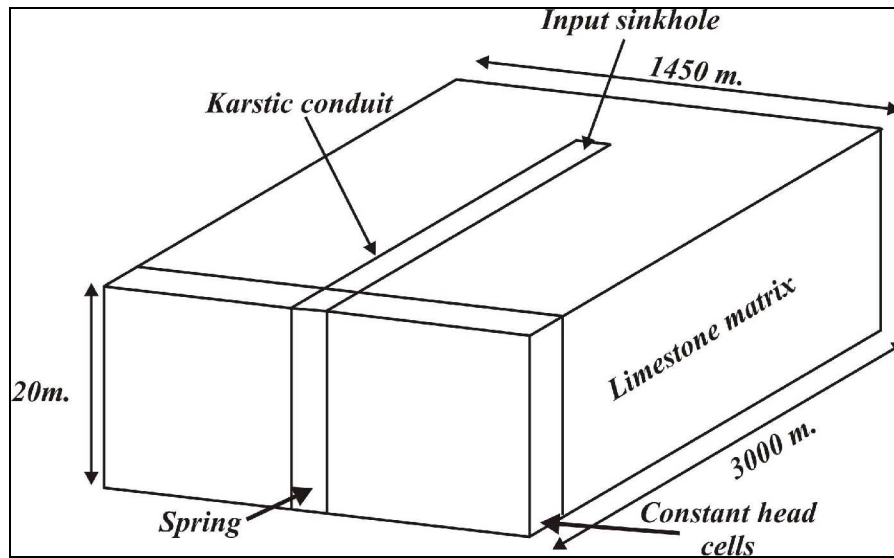


Figure 42. Sketch of the tested Model.

An event with allogenic ( $100 \text{ ls}^{-1}$  through sinkhole) and autogenic recharge ( $1 \cdot 10^{-5} \text{ mms}^{-1}$ ) was simulated.

The discharge was compared in laminar flow and turbulent flow with different Reynolds numbers.

Water discharge $\text{ls}^{-1}$	Laminar flow through conduit	Turbulent flow through conduit	Lower critical Reynolds number	Upper critical Reynolds number
142,3	Yes	No	-	-
16,2	No	Yes	20	30
46,4	No	Yes	200	300
130,1	No	Yes	2000	3000

Tab.8: Comparison of the spring discharge with different hydraulic regimes and different critical Reynolds numbers.

A brief comparison of the data in Table 8 indicates that MODFLOW-CFP yields lower discharge than MODFLOW for each couple of Reynolds number used. The turbulent flow tends to decrease the discharge by the friction to the conduits walls.

Another consequence is an increase of the water-table level in the aquifer.

That differences in discharge under turbulent flow condition means clearly that the Tanneben catchment need to have more water in input to provide the same discharge at the spring than in laminar flow.

## 7. Discussion about the potential intrinsic errors of modeling

During this work, a lot of assumptions were made in the modeling. Some of them are potentially erroneous. This aims to present them and to determinate whether they are important or not.

The first type of errors concerns the measurement errors. Indeed, data loggers and rain gauges can give such measurement errors due to negative temperature or snow fall. Normally, these kind of errors should have been corrected by the Joanneum Research Institute.

Another sort of errors concerns the frequency of sampling. In a perfect world, the data loggers should sample the discharge of the Lurbach, Hammerbach and Schmelzbach at the same time and with the same frequency. But in reality, they were sampled at different times and frequencies (Oswald, 2009): the discharge of Hammerbach, Schmelzbach and Lurbach cave were measured every 30 seconds, whereas the discharge of the upper Lurbach was monitored every 5 min at Lurbach station. This could be a problem to see the upper Lurbach maximum discharge during an event, because the Lurbach catchment produces Karst Flash Floods, where the water discharge increases very fast. This **aliasing effect** should be quantified and avoided, with an increase of the frequency of sampling, in order to make the monitoring at Lurbach station more reliable.

The third potential error involve the matrix specific storage. In all studies, the specific storage geometry was divided in two different areas: one for the Schmelzbach and one for the Hammerbach. This can be a rough approximation or an error to think that because the Hammerbach and Schmelzbach behave differently under various weather conditions, they have different storage capacities. A new investigation could be to determinate the difference between the specific storage assumptions used in this report and an homogenous matrix specific storage for the total Tanneben. Nevertheless the specific storage of the conduits should be still different of the specific storage of the matrix.

An important problem which should be noticed here was the approximation given in our models by the cell size of the conduits. To have a better computation of the models and a better precision, the conduits should have a low cell size. But as the conduits network was not drawn as straight lines, it was impossible to reduce the conduit cell size smaller than 100 m to 100 m. It could be possible to do that only with a one layer model, because this MODFLOW version allows only 12000 cells pro model. The problem encountered in this case is that the complex conduit geometry of the three and four layer models could not be implemented.

The last and biggest problem was to determinate which data are relevant in the data set to try to reproduce a correct behavior of the system. As we dispose of very few data and only one month data with all monitoring stations, it was hardly possible to exclude some data

Finally, the lack of information about the initial conditions and thus the need to make some assumptions (steady-state water table or hypothetical recharge event) is also a big source of errors. Some suggestions to prevent this are given in the following chapter.

## 8. Some suggestions for future work

Before the conclusion, we can claim that further work is necessary to have a better understanding of the system. Some questions, e.g. as to how the allogenic recharge infiltrates/percolates through the Tanneben massif and the Lurbach bed and how the infiltration sinkholes function, need to be solved.

An idea will be to use the allogenic character of the upper Lurbach to compute artificial discharge at the Lurbach station, using precipitation data of the surrounding with a predictive law such as **Gumbel** or a lumped model (rainfall-runoff model) using hourly parameters.

The Hammerbach discharge, Schmelzbach discharge and Lurbach (at Lurbach station and Lurbach cave) discharge need to be monitored in a longer period than that of the work by Oswald (2009). A minimum period of one year will be ideal to have a better idea of the seasonal behavior of the system. This could be also helpful to interpret existing data from Behrens et al. (1992), and Oswald (2009). More field investigations such as the mapping of the sinkhole network over the Tanneben massif and the improvement of the catchment delineation in the vicinity of the Badlgraben stream could also be helpful.

The infiltration of Lurbach water through sinkholes between the Lurbach station and the Lurbach cave need also be better understood and quantified under various weather conditions. Some field work such as tracer tests and discharge monitoring will be necessary to improve this knowledge.

Another idea will be to try to compute the lacking input data with the output data. Some interesting papers provide methods to find precipitation and discharge at entrance of the system based on the output discharge.

- Geyer et al. (2008) provide a method which uses the first (and sometimes second) time derivative of the spring discharge to identify the recharge function. This method further needs a recession coefficient of the highly conductive conduit system, which can be obtained from the evaluation of the hydrograph recession or tracer tests.
- Covington et al. (2009) provides a method describing the effects of recharge and geometry on discharge of simple karstic aquifers.

In this report, no investigation about the Hammerbach threshold effect was presented. This should be implemented in a future research, only if more available field discharge data sampled under various weather conditions are as disposal.

All of this suggestions may help solving or understanding some of the unanswered questions:

- has the Lurbach system a new behavior since 2005 or not?
- is the threshold effect between Hammerbach and Schmelzbach still active?
- what about the possibilities of another flow path from the Lurgrotte to the Hammerbach

## Conclusions

In spite of several difficulties of discrete modeling in karstified lands, this report can give some interesting conclusions.

The modeling of a karst aquifers with MODFLOW is possible under several conditions:

- the conduit network should be really well known. Several geometrical assumptions should be tested before the choose of one particular geometry.
- the steady-state can give very good results, even so karstic aquifers are rarely in steady-state.
- input and output data must be available for a sufficient period of time. This allows to determine precisely the behavior of the system under various weather conditions and thus to provide a basis for modeling assumptions. If no input data are available some numerical methods can be helpful to simulate them.

Turbulent flow should be integrated if the possibilities allow it. Thus, CFP should be further improved to allow a simulation in turbulent flow for more complex, realistic models.

## References:

- Bakalowicz, M., (2005): Karst groundwater: a challenge for new resources.
- Behrens, H., Benischke, R., Bricelj, M., Harum, T., Käss, W., Kosi, G., Leditzky, HP., Leibundgut, C., Małoszewski, P., Maurin, V., Rajner, V., Rank, D., Reichert, B., Stadler, H., Stichler, W., Trimborn, P., Zojer, H. & Zupan, M., (1992): Investigations with Natural and Artificial Tracers in the Karst Aquifer of the Lurbach System (Peggau-Tanneben-Semriach, Austria).- Steirische. Beiträge. zur Hydrogeologie, 43, 9-158, Graz.
- Bonacci, O., Ljubenkov, I. & Roje-Bonacci, T., (2006): Karst flash floods: an example from the Dinaric karst (Croatia).
- Cornaton, F., & Perrochet, P., (2002): Analytical 1D dual-porosity equivalent solutions to 3D discrete single continuum models. Application to karstic spring hydrograph modelling.
- Covington, M. D., Wicks, C. M. & Saar, M. O., (2009): A dimensionless number describing the effect of recharge and geometry on discharge from simple karstic aquifers.
- Cvijić, J., (1893): Das Karstphänomen: Versuch einer morphologischen Monographie, Wien, 113 S. (Geographische Abhandlungen, hrsg. von Prof. Dr Albrecht Penck. V, Heft 3).
- Darnault, C. J. G., (2008): Karst aquifers: Hydrogeology and exploitation. Overexploitation and Contamination of Shared Groundwater Resources. Springer Science.
- Filipponi, M., (2009): Spatial analysis of karst conduit networks and determination of parameters controlling the speleogenesis along preferential lithostratigraphic horizons.
- Fleury, P., Plagnes, V., & Bakalowicz, M., (2007): Modeling of the functioning of karst aquifers with a reservoir model: Application to Fontaine de Vaucluse (South of France).
- Ford, D., & Williams, P., (2007): Karst Hydrogeology and Geomorphology. John Wiley & Sons, Ltd.
- Geyer, T., Birk, S., Liedl, R. & Sauter, M., (2007): Quantification of temporal distribution of recharge in karst systems from spring hydrographs.
- Gray, D., M., (1970): Handbook on the Principles of Hydrogeology. -Secretariat Canadian Nat. Com. for the International Hydrological Decade, Ottawa.
- Jukić, D., & Denić-Jukić, V., (2009): Groundwater balance estimation in karst by using a conceptual rainfall-runoff model.
- Klimchouk, A., & Andrejchuk, V., (1996): Sulphate rocks as an arena for karst development.
- Mangin, A., (1974.a): Contribution à l'étude hydrodynamique des aquifères karstiques. Annales de spéléologie (in French).
- Marsaud, B., (1996): Structure et fonctionnement de la zone noyée des karsts à partir des résultats expérimentaux. (Structure and functioning of the saturated zone of karsts from experimental results). (Doctorate Thesis in French, Paris XI, Orsay, 305 pp).

- Maurin, V., (1952): Ein Beitrag zur Hydrogeologie des Lurhöhlensystems - Die zweite Chlorierung des Lurbaches (in German).
- Maurin, V., (1954): Das Paläozoikum im Raum zwischen Deutschfeistritz und Semriach Beiträge zur Kenntnis des Grazer Paläozoikums III\*) (in German).
- Oswald, S., (2009): Künstliche und natürliche Tracer in einem Karsteinzugsgebiet mit allochtoner Neubildung (Lurbach, Österreich) (in German).
- Reimann, T., Birk, S., Rehr, C.(†), & Shoemaker, B., (2010): Modifications to the conduit flow process mode 2 for MODFLOW-2005.
- Salomon, J. N., (2006): Précis de Karstologie. Seconde édition. Presse universitaire de Bordeaux (in French).
- Sauter, M., Kovács, A., Geyer, T., & Teutsch, G., (2006): Modellierung der Hydraulik von Karstgrundwasserleitern - Eine Übersicht (in German).
- Schwinner, R., (1925): Das Bergland nordöstlich von Graz. Sitzungsber. Akad. Wiss., math-naturwiss. Kl. (I) 134, 219-276, Wien (in German).
- Shoemaker, W.B., Kuniandy, E.L., Birk, S., Bauer, S., Swain, E.D. (2008): Documentation of a Conduit Flow Process (CFP) for MODFLOW-2005. U.S. Geological Survey Techniques and Methods 6-A24.
- Teutsch, G., & Sauter, M., (1991): Groundwater modeling in karst terrains: Scale effects, data acquisition and field validation.
- White, W. B., & White, E. L., (2005): Groundwater flux distribution between matrix, fractures, and conduits: constraints on modeling.
- Worthington, S., R., H., (2007): Groundwater residence times in unconfined carbonate aquifers.